

# **Automated Design Process of Sustainable Industrial Packaging**

by

CHING-JUI CHANG

A Dissertation submitted to the

Graduate School-New Brunswick

Rutgers, The State University of New Jersey

in partial fulfillment of the requirements

for the degree of

Doctor of Philosophy

Graduate Program in Mechanical and Aerospace Engineering

Written under the direction of

Professor Hae Chang Gea

and approved by

---

---

---

---

New Brunswick, New Jersey

May, 2007

# **ABSTRACT OF THE DISSERTATION**

## **Automated Design Process of Sustainable Industrial Packaging**

By CHING-JUI CHANG

Dissertation Director:  
Professor Hae Chang Gea

Sustainability and environmentology are becoming important issues because the natural resources have been heavily consumed in the past century and major parts of them have been wasted on some one-time-use type of applications such as packaging. As an engineer, and more basically as a resident of our only earth, one is obligated to preserve the natural resources for the coming generations. One should not selfishly consume the limited natural resources found on the earth but should use these with appreciation of what we have been given. Designs for sustainability and environmentology in industrial packaging are studied in this research by means of reducing unnecessary usage of material, increase structure strength under limited amount of material and replacing plastics with environmentally friendly materials. These ideas are accomplished by incorporating some design concepts on generating new packaging structures. These designs include design of the core structures of sandwich board, design of supporting tray efficiently, and design of molded pulp with better reinforcements. Topology optimization of packaging structures utilizing environmental friendly materials is also studied in this dissertation to determine a set of packaging with less material while

strength of the packaging structure is optimized; and less pollution and impact on the environment is accomplished.

The main contributions of this dissertation are: (1) Design toward sustainability and environmentology, (2) Developed a simple topology optimization scheme that provides valid results to design spaces with non-uniform element volume, (3) Development of automatic and efficient mold design algorithm for general supporting packaging, (4) Application of topology optimization to the design of industrial packaging, and (5) Development of systematic design process of designing molded pulp.

## **Acknowledgement**

I would like to express my deepest appreciation to my advisor Prof. Hae Chang Gea for his valuable guidance and continuous encouragement throughout my doctoral studies. His friendly advice and high degree of motivation have been very helpful to my academic and personal aspects of my life.

I would also like to thank my committee members, Prof. Noshir A. Langrana, Prof. Alberto Cuitino and Prof. Elsayed A. Elsayed, for their interest in this research and for their valuable time in reviewing this dissertation.

I wish to acknowledge my fellow graduate students and friends for their help and friendly company. In particular I wish to thank Bin Zheng, Po-Ting Lin, Cheng-Chung Lee, Kunja Oza, and Paritosh Khobare.

I am extremely grateful to my family members for their enormous encouragement during these years. It would not be possible without their support.



# **Dedication**

To my wife Shu-Ju  
and parents

# Table of Contents

<b>Abstract.....</b>	<b>ii</b>
<b>Acknowledgement.....</b>	<b>iv</b>
<b>Dedication.....</b>	<b>v</b>
<b>Table of Contents.....</b>	<b>vi</b>
<b>List of Figures .....</b>	<b>viii</b>
<b>List of Tables .....</b>	<b>xii</b>
<b>Chapter 1. Introduction .....</b>	<b>1</b>
1.1    Review of Research in Industrial Packaging .....	6
1.2    Review of Research in Structural Optimization .....	8
1.3    Research Contributions .....	11
1.4    Outline of the Dissertation .....	13
<b>Chapter 2. Design of Core Structures of Sandwich Board.....</b>	<b>17</b>
2.1    Introduction.....	17
2.2    Problem Formulation .....	21
2.3    Microstructure Based Composite Material Models .....	23
2.3.1    Solid Isotropic Microstructure with Penalty Model.....	24
2.3.2    Spherical Micro-inclusion Model .....	27
2.4    Optimization Algorithm Using Optimality Criteria.....	29
2.5    Examples.....	34
2.5.1    Example 1: A Short Cantilever Beam.....	34
2.5.2    Example 2: A 3D Cantilever Beam .....	35
2.6    Optimization of Core Structure of Sandwich Board.....	37
2.6.1    Design 1: A Single Cell Sandwich Structure.....	38
2.6.2    Design 2: A Multiple Cell Sandwich Structure .....	39
2.6.3    Design 3: A Thin and Long Sandwich Beam .....	41
2.7    Conclusion and Remarks .....	43
<b>Chapter 3. Design of Packaging Supporting Tray .....</b>	<b>45</b>
3.1    Introduction.....	45

3.2	Packaging Supporting Space Identification .....	49
3.2.1	Facet Reduction .....	50
3.2.2	Height Detection .....	54
3.2.3	Surface Generation.....	58
3.3	Examples.....	61
3.3.1	Example 1: A Ball Model .....	61
3.3.2	Example 2: A Suspension Model of a Remote Controlled Car .....	63
3.3.3	Example 3: A Dragon Model.....	64
3.4	Efficiency Tests .....	65
3.5	Conclusion and Remarks .....	68
<b>Chapter 4. Design of Thin-walled Packaging Structures .....</b>		<b>70</b>
4.1	Introduction.....	70
4.2	Benefits of Using Molded Pulp.....	73
4.3	Challenges to Molded Pulp.....	75
4.4	Obtaining Design Space.....	78
4.5	Applying Topology Optimization.....	80
4.6	Design Examples .....	81
4.6.1	Example 1: A Simple Box Model.....	81
4.6.2	Example 2: A Toy Car Model.....	84
4.7	Conclusion and Remarks .....	88
<b>Chapter 5. Conclusion and Future Work.....</b>		<b>89</b>
5.1	Conclusion .....	89
5.2	Future Work .....	91
<b>Bibliography .....</b>		<b>93</b>
<b>Curriculum Vita.....</b>		<b>98</b>

# List of Figures

Figure 1-1: Time Table for Commonly Used Materials to Biodegrade. (Source: The Coral Reef Alliance & Worldwide).....	3
Figure 1-2: Plastics Produced and Recycled in United States in 2001. (U.S. EPA) .....	4
Figure 1-3: A typical Sandwich Structure. (Source: <a href="http://www.talasonline.com">http://www.talasonline.com</a> ) .....	13
Figure 1-4: Typical Molded Tray Used in Packaging. (a) Molded Foam. (Source: <a href="Http://www.knauf-eps.com">Http://www.knauf-eps.com</a> ) (b) Molded Thin Film Tray. (Source: <a href="https://www.impact-mfg.com">https://www.impact-mfg.com</a> ).....	15
Figure 1-5: A Typical Molded Pulp Packaging as a Tray to Hold Products in Position. (Source: <a href="http://www.pacificpulp.com">http://www.pacificpulp.com</a> ).....	16
Figure 2-1: Some Commonly Seen Core Structures of Cardboard. [21] (a) Cross Corrugation. (b) Trapezoidal Corrugation. ....	19
Figure 2-2: Design Domain of Typical Topology Optimization Problem. ....	21
Figure 2-3: Penalization of the Intermediate Volume Densities in SIMP Model [25]. ....	24
Figure 2-4: A Comparison of the SIMP Model and the Hashin-Strikhman Upper Bound for an Isotropic Material With Poisson Ratio $\nu = 1/3$ mixed with void. For the H-S Upper Bound, Microstructures With Properties Almost Attaining the Bounds Are Also Shown. [27] .....	26
Figure 2-5: Microstructures of Material and Void Realizing the Material Properties of the SIMP Model With $p = 3$ , for a Base material With Poisson's Ratio $\nu = 1/3$ . As Stiffer Material Microstructures Can Be Constructed From the Given Densities, Non-structural Areas Are Seen at the Cell Centers. [27].....	26
Figure 2-6: Microstructure of the Spherical Micro-inclusion Material Model.[28].....	27
Figure 2-7: Relative Stiffness vs. Volume Fraction for the Spherical Micro-inclusion Model and the SIMP Model With Penalization Power $p = 2$ . ....	28
Figure 2-8: A Short Cantilever Beam Is Subjected to a Vertical Load in the Middle of the Right Side and Clamped on the Left Side. ....	35
Figure 2-9: The Result of the Short Cantilever Beam Subject to the Boundary Conditions Shown in Figure 2-8. ....	35

Figure 2-10: A 3D Cantilever Beam Is Subjected to a Vertical Load at the Center of its Right Bottom Edge with its Four Left Corners Fixed. ....	36
Figure 2-11: The Optimal Topology of the 3D Cantilever With the Boundary Conditions Shown in Figure 2-10. ....	36
Figure 2-12: Top View and Front view of the Same Result Shown in Figure 2-11.....	37
Figure 2-13: Sandwich Board Strength Test Setup. (Source: Industrial and System Engineering Dept. at Rutgers Univ.).....	38
Figure 2-14: (a) Single Cell Design Space of a Sandwich Board. Left is fixed while right is rolling. A force is placed at the upper right corner. The volume constraint is 10 percent (b) Topology Optimization Result.....	39
Figure 2-15: Mirrored Topology Optimization Result of the Single Cell Design to Show the Whole Design.....	39
Figure 2-16: Design Space of Multiple Cell Sandwich Structure.....	40
Figure 2-17: Topology Optimization Result. Upper and lower layers are set to be non-designable with densities to be 0.3 and the volume constraint is 10 percent.....	40
Figure 2-18: Mirrored Topology Optimization Result of Multiple Cell Design to Show the Whole Design.....	41
Figure 2-19: Design space of a Long Sandwich Board Structure Divided into 200 x 40 Elements.....	42
Figure 2-20: Historiography Data of the Long Sandwich Board Design.....	42
Figure 2-21: Final Topology Optimization Result of the Long Sandwich Board. 10 percent of the volume is specified to be the upper limit. ....	43
Figure 2-22: Topology Optimization Result of Long Sandwich Design to Show the Whole Design.....	43
Figure 2-23: 3D Visualization of the Sandwich Design Presented and Discussed in This Section. [21].....	43
Figure 3-1: Examples of Supporting Tray. (a) Polyurethane foam tray. ( <a href="http://www.gwwcases.com">http://www.gwwcases.com</a> ) (b) Thin film plastic tray. ( <a href="http://www.arrowheadinc.com">http://www.arrowheadinc.com</a> ) .....	46
Figure 3-2: Boolean Operation May Create Faulty Design for Concave Models (a) Faulty Design. (b) Valid Design.....	49
Figure 3-3: Expected Height Detection Result Indicated in Red Dots. ....	51
Figure 3-4: Triangle Primitive of a 3D Model in the STL File Format. ....	52

Figure 3-5: All Facets With Green Normal Vectors Should not be Included in the Intersection Test. ....	53
Figure 3-6: Grids Enclosed by a Projected Facet along the Supporting Direction.....	54
Figure 3-7: Top View of the Projected Triangle of the Base of the Height Grid Mesh. ....	55
Figure 3-8: Edge Vector and the Vector Formed by the End Vertex and Targeting Grid Are Used in the Inner Test. ....	56
Figure 3-9: Height Adjustment when Multi Crossing Cases Occurs to Avoid Undercut. ....	57
Figure 3-10: (a) Direct Connecting of Mesh Grids Results in Minor Undercut. (b) Height Relaxation Can Avoid This Effect.....	58
Figure 3-11: (a) Sharp Edges Exists on the Connected Surface. (b) Sharp Edges Reduced After Applying Smoothing Filter. ....	59
Figure 3-12: A Smoothed Connected NURBS Surface Is Shown as the Green Line.....	60
Figure 3-13: (a) A ball model with 1596 facets, (b) Supporting space for a bounding box with height of 45% of the diameter of the ball, and (c) Supporting space for a bounding box with height of 70% of the diameter of the ball.....	62
Figure 3-14: (Left) A Suspension Model. (Right) A Closer Cut-away View of the Internal Components .....	63
Figure 3-15: (A) Suspension Model and Supporting Space with 70% Height, (b) Supporting Surface.....	63
Figure 3-16: A Dragon Model with Flat Base Facing Down.....	64
Figure 3-17: Efficient Test Results on Different Number of Facets of the Same Ball Model.....	65
Figure 3-18: Efficient Test Result on Ball Models with Different Number of Supporting Base Grids. ....	67
Figure 3-19: Efficiency Test Results on Different Models.....	68
Figure 4-1: An Example of Molded Pulp for a Printer. ( <a href="http://www.enviropak.com">http://www.enviropak.com</a> ).....	70
Figure 4-2: Process of Making Molded Pulp.....	72
Figure 4-3: A Picture Showing Space Saving Feature of Molded Pulp. ( <a href="http://www.enviropak.com">http://www.enviropak.com</a> ).....	74
Figure 4-4: The (a) Forming Mold and the (b) Mesh that Will Be Added onto it. ....	77

Figure 4-5: An Illustration of HEX8 / CHEXA Element Defined in Nastran Bulk Format.....	78
Figure 4-6: An Example of Continuous Mesh for a Simple Box Model. ....	79
Figure 4-7: An Example of Forming a Thin and Continuous Connected FEA Mesh Layer.....	79
Figure 4-8: A Box Example of Topology Design Space Detection. ....	82
Figure 4-9: Topology Optimization Result for the Box Model. (a )& (b) Design Space. (c) Result of Locations to Add Reinforcements. (d) Result with Material Densities Less Than 0.1 Removed. ....	83
Figure 4-10: Height Detection and Design Space Generation for a Car Model. ....	85
Figure 4-11: Result of Topology Optimization for a Car Model: (a) & (c) Result of locations to add reinforcements. (b) & (d) Result of locations to add reinforcements with material densities less than 0.1 removed.....	86
Figure 4-12: Result of Topology Optimization for a Car Model Under Different Boundary Conditions: (a) & (c) Result of locations to add reinforcements. (b) & (d) Result of locations to add reinforcements with material densities less than 0.1 removed.....	87

## List of Tables

Table 1: Efficiency Test Result of a Simpler Ball Model with Different Grid Configurations .....	66
Table 2: Efficiency Test Result of a Complex Ball Model with Different Grid Configurations. ....	67
Table 3: Efficiency Test Result of a More Complex Dragon Model with Different Grid Configurations. ....	68



# **Chapter 1.**

## **Introduction**

The human economy is generally based on fabricating, transporting, selling, and buying, thus, all types of goods require proper packaging in order to transport the product from the manufacturer to the retailer, and eventually to the customer. The importance of packaging has significantly grown during the past few decades. One seldom realizes how much modern technique is required to produce a satisfactory package in order to achieve the desired specification. Packaging technologies not only provide product protection but also enhance product presentation. Well-designed and well-constructed packaging can deliver better transportability and consequently increase product values.

In terms of increasing product value, elaborate packaging enhances the product value by presenting them in a specific way that impresses the customers. Another important purpose of packaging is marketing. Attractive packaging will help draw more customers and will encourage more purchases of the product. The customers usually learn about the products from commercial advertisement. In addition to the advertisement, the presentation of the products in the package is another reason for customers to purchase the item because the way they are presented makes the potential buyers consider if they want or need the products and eventually purchase them. Hence, the packaging virtually promotes the products' value. The product and the package are becoming so interdependent that we cannot consider one without the other. Decorative

packaging is a level of art and its value really depends on the prospective aspect of the manufacturer and the customers. Thus there is very little research applied on this field to date.

In terms of delivering better transportability, proper protective packaging provides abilities of vibration absorption and shock resistance, etc. so that the products can be delivered without damage. During the transportation process, the products experience vibrations that come from the unexpected rough road surfaces, drivers' unprofessional driving skills. The products also suffer from shocks due to careless handling of moving and throwing from one place to another or from some unanticipated accidents. Some products are temperature sensitive hence the temperature needs to be maintained within a given range. With proper design considerations and implementation, all those protection requirements can be achieved using appropriate materials and technologies.

However, most packaging materials are one-time-use type that will be deposited to landfill if recycling of such material is not possible or not well developed. Plastics are commonly used since the industrial revolution because of their well developed manufacturing processes and some outstanding material properties such as great acid / alkaline resistance, long durability, etc. When plastics are used to fabricate consumer products such as cell phone cases, their lifespan is expected to be longer, usually from months or up to several years. Nevertheless, when it comes to packaging, the lifespan is considerably shorter, typically days to weeks. If these packaging plastics are not recycled as designated, they are generally thrown into trash cans and eventually dumped into landfills and will take a very long period of time to degenerate. Figure 1-1 shows a chart of time required for commonly used materials to biodegrade. It can be easily seen

that plastics take the longest time to degenerate, especially those used for packaging. It can take up to one thousand years or longer for plastic bags to biodegrade. On the other hand, paper products only require up to five months to biodegrade.

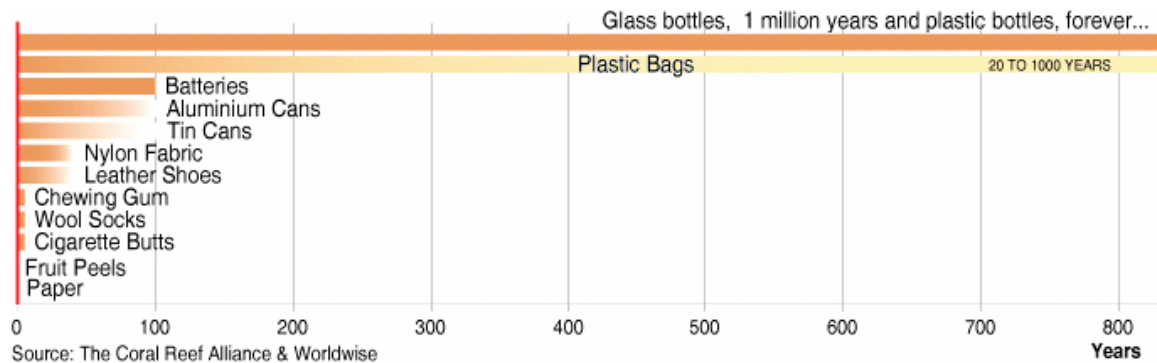


**Figure 1-1: Time Table for Commonly Used Materials to Biodegrade.**  
(Source: The Coral Reef Alliance & Worldwise)

Most developed countries have carried out recycling policies targeting this plastic polluting problem with little success. Pollution has been a serious problem since the development of petroleum industry in twentieth century. Plastics and polymers are some of the main pollution sources. A great part of plastics and polymers is used for merchandise packaging including food, general goods, industrial packaging, etc. Earlier in the end of last century, U.S. Environmental Protection Agency (EPA) and other environmental groups were propagandizing the concept of recycling as well as developing some acts in order to reduce pollution and reuse some of the petroleum production. However, only a portion of the plastics can be reprocessed for other purposes because people are putting recyclable materials into general garbage bags so that the effect is very limited [1, 2]. That is why plastics are the most common objects to be seen in the landfill. Figure 1-2 shows the recycling amount of plastics in United States in the year 2001. It can be seen that the recycled amount is far behind the amount produced. Actually, the plastic recycling rate keeps declining in the last few years of

twentieth century as well as the beginning of this century according to the EPA. Thus, some environmental friendly materials should be widely used to replace those non-fully recyclable materials, especially those one-time-use packaging materials.

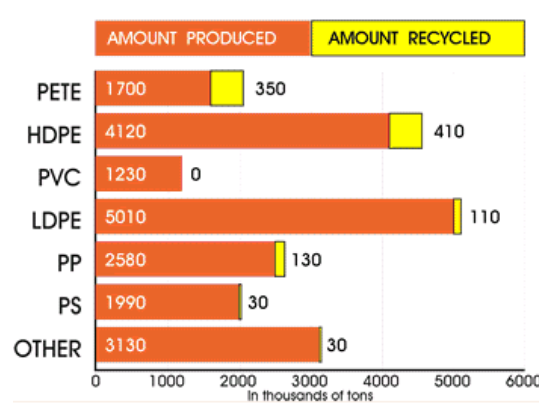


*Figure 1-2: Plastics Produced and Recycled in United States in 2001. (U.S. EPA)*

There are two major approaches to solve this problem toward sustainability: (1) search substitute material that is environmental friendly to replace plastics, and (2) improve material efficiency by finding stiffer structures that require less material. In the first approach, the new material has to be biodegradable in a shorter time frame and to be safe to be dumped to landfill. It would be a plus if the new material can be made from substances that were considered waste originally. However, this approach requires more time and budget to search appropriate substances and takes even more time and cost to release to the market. In the second approach, existing environmental material such as paper is considered to be the base material. Stiffer structures are designed, simulated, and verified based on the chosen material. This approach is based on known technologies and materials and consumes less budget and time to accomplish.

As an example to the first approach, Cargill Dow's PLA (polylactic acid) is introduced here. PLA produced by Cargill Dow uses corn starch as a feedstock. Corn is milled, which separates starch from the raw material. Unrefined dextrose is then processed

from the starch. Dextrose is turned into lactic acid using fermentation, similar to that used by beer and wine producers. Through a chemical process called condensation, two lactic acid molecules are converted into one cyclic molecule called a lactide. This lactide is purified through vacuum distillation. A solvent-free melt process causes the ring-shaped lactide polymers to open and join end-to-end to form long chain polymers. A wide range of products that vary in molecular weight and crystallinity can be produced, allowing the PLA to be modified for a variety of applications. [3]

Although scientists and engineers have done much research on the new material to replace the plastics used nowadays, they are facing difficulties on massive production of the new materials due to the technology bottleneck. If some material, which is currently greatly available, recyclable, and environmental friendly, can be engineered to have better mechanical strength, then it can be used to replace some applications that are currently using plastics. The most possible one is using paper or paper pulp to replace plastic packaging since the packaging is one-time-only usage and plastics takes literally forever to degenerate when others take a much shorter amount of time. Paper products usually take less than six months to biodegrade (Figure 1-1). This fact makes paper a perfect candidate to replace plastics in packaging.

In the second approach, finding stiffer structures that utilize less material is the main task. Some known stiff structures or stiffeners are studied and applied to different fields and scenarios. In industrial packaging field, some common primitives of packaging such as sandwich board, corner protectors, and pallet are studied. However, the core structure in those primitives are usually using some known pattern and optimized by varying some pre-defined parameters which can not guarantee global optimal. It is very infrequent to

see the application of topology optimization methods on packaging primitives and structures. Thus, this study attempts applying linear topology optimization methods on designing packaging structures from small cell scale of a packaging element to a full scale packaging structure using paper and paper pulp. Reviews of industrial packaging and structural optimization are discussed in the following sections to provide a fundamental overview on these topics.

## **1.1 Review of Research in Industrial Packaging**

Packaging is the process of placing objects, generally commercial products, into a container. Packaging serves a variety of purposes for both the producer and the consumer. The most obvious purpose of packaging is to physically protect the products from shocks and vibrations during transportation and warehousing processes which usually plays the major role of damaging the products. Packaging can be made to protect the product from extreme heat and cold. It can also protect the product from weather, such as rain and sunlight, during transport. In addition, packaging can protect the product from being contaminated by airborne pathogens or from being damaged by handling or pressure. Packaging also aids in the grouping of small objects for efficiency. For example, placing 1,000 finishing nails inside one package makes it easier to transport the nails than if they were packaged individually. Packaging can also help transform bulk commodities into sizes that are more suitable for individual use. Packaging also aids in the reduction of theft. Some packages, for example, are purposely made to be much larger than the object inside. This is commonly seen in software packages, where the packaging for the software is much larger than the disc being housed inside. This

larger packaging makes it more difficult for a thief to hide the product and remove it from the store.

Packaging methods can be categorized as two types: free format and fixed format. In the free format packaging, there is no predefined form or shape for packaging materials, and the product is loosely surrounded and protected by some flexible packaging materials. Free format packaging cannot utilize the packaging materials and space very efficiently therefore it is not normally used for massive industrial packaging. The fixed formats can be categorized to some primitives such as cardboard (as known as corrugated core sandwich panels, or corrugated board; sometimes made with plastics), corner protector, stack separator, foam protector, pallets, etc. However, only a few of them are intensively studied in terms of their mechanical structure strength and further optimization. The most common packaging material studied in the mechanical aspects is cardboard, a sandwich panel structure. In 2003, Qiu et al. [4] studied a sandwich beam subject to shock loading using the finite element method (FEM). In 2004, Fleck and Deshpande [5] presented the response of a sandwich beam with different sandwich cores subjected to a load analytically. Some studies applied optimization methods to refine existing shapes of sandwich core, such as Hohe and Becker [6] in 2002; and Valdevit et al. [7] in 2004.

Nevertheless, no further studies can be found on studying other packaging structures. There is still large amount of research to be studied on this field. Topology optimization is used in this study to optimize packaging structures. The review of structural optimization is discussed in the following section.

## 1.2 Review of Research in Structural Optimization

Essential components of structural optimization were first established and made possible centuries ago by Galileo Galilei (1564-1642) who performed systematic investigations into the fracture process of brittle bodies, and Robert Hooke (1653-1703) who formulated the fundamental law of the linear theory of elasticity: Strain and stress are proportional to each other [8]. The field of structural optimization was initially investigated over one hundred years ago. The first theoretical work was attributed to Maxwell (1869) [9], who justified that for a fully stressed pin jointed framework with a given set of forces applied at specified locations, the volume difference between tension and compression members is a constant. In 1904, based on Maxwell's result, Michell [10] proposed a general theory for minimum weight structures. These works provided a theoretical basis of structural optimization.

During the late 1940s and 1950s, a great amount of research was put into the development of minimum weight design for aircraft structural components. Two intuitive Optimality Criterion (OC) [11] methods for structural design were developed in this era: Simultaneous Failure Mode Design (SFMD) and Fully Stressed Design (FSD). SFMD is based on the assumption that if the optimal structure is overloaded, two or more modes of failure will occur simultaneously. Shanley (1960) [12] applied this principle to many optimization problems in aircraft structural component designs. On the other hand, the FSD method considered that the stress in each member of the optimal structure is equal to the maximum allowed stress. This method produces the minimum weight design only when the structure is statically determinate and subject to a single concentrated load (Gallagher 1973 [13]). The theoretical foundation of the OC



approach was established by Prager and Taylor (1968) [14] and Sheu and Prager (1968) [15]. They showed that some continuum problems lead to differential equations as the optimality criteria and the solution of the differential equations define the optimal shape of the structure. However, the OC approach is not a general method since the optimality conditions must be derived on a case by case basis, which limits the range of its applications.

Mathematical Programming (MP) methods, the Finite Element Method (FEM) and computer technologies have made it possible to generalize and simplify the problems and extend the application to larger problem sizes. In terms of mathematics, it is of utmost to mention Leonard Euler (1707-1783) who has played a most significant scientific role in developing the theory of extremals which provide the fundamentals for the development of the calculus of variations. With this method, Jakob Bernoulli (1655-1705) determined the “curve of the shortest falling time” (Brachistochrone) and Sir Isaac Newton (1643-1727) determined the body of revolution with the smallest resistance. By formulating the principle of the smallest effect, and by developing an integral principle Lagrange (1736~1813) and Hamilton (1805~1865) contributed toward the completion of variational calculus as one of the fundamentals for several types of optimization problems. In those problems, optimality criteria are derived as necessary conditions. In the case of unconstrained problems Euler equations are used. Constraints are considered by applying the Lagrangian multiplier method. In addition to the mathematical tools, the finite element method made it possible to construct complex problems and approximate it into generalized finite elements such that it can be determined by solving a set of simultaneous linear equations. However, it is not

possible to perform topology optimization without the design sensitivity analysis. Design sensitivities serve mainly as an indicator for measuring how well a small perturbation of design variables will affect the system response or the objective function of optimization. Based on the information obtained from design sensitivities, the optimum design can be determined by using optimization algorithms. There are two fundamentally different approaches to compute design sensitivities: the discrete approach and the variational approach. The first approach uses the discretized model, based on finite element analysis, to carry out the analysis by perturbing each design variable in turn. It has three different computational methods: the analytical method, the semi-analytical method, and the finite difference approximation [16, 17]. With the availability of high speed computers and efficient linear algebra algorithms, structural optimization was adopted as a design tool and has been implemented in many Computer Aided Engineering (CAE) systems.

Topology optimization of continuum has been developed on top of finite element analysis and sensitivity analysis, and has been successfully applied to many structural design problems such as design of the stiffest structures, design of compliant mechanisms, and design of structures with maximum eigen-frequencies. Many nonlinear problems were transformed into a set of approximation sub-problems based on mathematical derivations or physical assumptions. Various optimization methods have been developed and studied for acquiring the optimal design. Among those algorithms, the most commonly used algorithms are the Sequential Linear Programming (SLP), feasible directions, various sequential unconstrained minimization methods, generalized geometric programming, steepest descent, conjugate gradient and dynamic programming in

conjunction with the penalty method. A detailed comparison and discussion of these methods can be found in Gallagher and Zienkiewicz (1973) [13], Carpenter and Smith (1977) [18], Schittkowski (1985) [19], and Belegundu and Arora (1985) [20].

The objectives of this dissertation are to design stiffer structures of packaging primitives and develop automated methods to generate packaging structures that can accommodate a given set of products / objects. In order to accomplish these goals, some supportive methods are studied and developed. They include (1) developing topology optimization procedures suitable for packaging applications, (2) obtaining appropriate design space for finite element analysis and topology optimization processes, and (3) defining suitable boundary conditions to obtain useable results. Some of the main contributions of this study are mentioned in the following section.

### 1.3 Research Contributions

The main contribution of this dissertation is (1) the application of topology optimization to the design of industrial packaging, (2) the development of automatic mold design for general supporting packaging, and (3) the development of systematic design process of designing molded pulp. Several achievements are summarized as below:

- ***Design toward sustainability and environmentology.***

Sustainability is generally defined as “Meeting the needs of the present without compromising the ability of future generations to meet their own needs” and environmentology is defined as “a systematized science whose purpose is that human beings control their activities suitably in the limited Earth”. These subjects have become more and more important recently. This study considers using paper as a base

material to construct packaging structures in order to reduce plastic wastes while providing an outstanding solution.

- ***Analysis and application of topology optimization with a simple variable updating scheme***

An analysis of optimality criteria has been studied and a simple design variable updating scheme is constructed considering the sensitivity of energy density. The sensitivity analysis is used as an indicator of how significant a design variable can modify the current design. This method provides a simple scheme to compose an efficient computer program for topology optimization.

- ***Topology optimization of the elements of industrial packaging***

The Topology optimization method is used to design some packaging. They are modeled and some optimized result are presented and discussed. First, core structure of sandwich structure is designed in chapter 2. Then, an efficient method of obtaining supporting surface that can be used to generate thin film package is designed in chapter 3. Finally, mold pulp is designed in chapter 5 using the methods described in other chapters.

- ***Automated mold design of supporting packaging surface***

A simple yet efficient algorithm has been constructed to generate a supporting packaging surface that can be used to form molded foam or thin film tray. It takes models in a commonly used file format as input and exports an undercut-free supporting bulk as a stereolithography (STL) file format which can be easily built by rapid prototyping (RP) machines or computer numerical controlled (CNC) machines.

- ***Topology optimization of thin-walled packaging structure***

The topology optimization method has been used to indicate portions on a thin-walled supporting film to be reinforced. It can be used to create molds for molded pulp for packaging.

## 1.4 Outline of the Dissertation

This dissertation consists of five chapters covering packaging materials and structures in mechanical aspects by a bottom-up approach. Three types of packaging structures are studied. They are core structure of sandwich board, molded supporting foam, and molded pulp. All the details are introduced and discussed in the rest of the dissertation. The remainder of this dissertation is organized as follows:

In chapter 2, core structures of sandwich board are studied. A typical sandwich board structure is shown in Figure 1-3. The objective in chapter 2 is to design a stiffest core structure in a region that is covered by an upper and a lower of material with given strength. There is no pre-defined core structure pattern to limit the final result. Thus all the space between the given layers is designable. This problem is well-known as structural optimization problem.



*Figure 1-3: A typical Sandwich Structure. (Source: <http://www.talasonline.com>)*

In order to obtain the core structure, topology optimization method is selected to handle this design task. In this chapter, elements of topology optimization such as problem formulation, material model, sensitivity analysis, and optimization method are discussed. A simple design variables updating scheme for minimum mean compliance topology optimization problem is constructed based on optimality criteria and sensitivity analysis. This method provides more condensed topology results without smaller features that are not easy to fabricate. A number of examples generated by this method are presented and discussed in chapter 2. Then design spaces for the sandwich board are sent to the topology optimization algorithm composed in chapter 2. The sandwich board is modeled using a long sandwich beam to obtain the sandwich core that can increase the stiffness. Possible applications of this sandwich board in addition to packaging are also discussed in chapter 2.

In chapter 3, molded supporting bulk / surface for packaging is studied. The molded foam is usually used as a tray to hold products in desired positions in order to provide protections to the products. Commonly seen molded foams and thin-film packaging are shown in Figure 1-4.



**Figure 1-4: Typical Molded Tray Used in Packaging.**  
**(a) Molded Foam.** (Source: [Http://www.knauf-eps.com](http://www.knauf-eps.com))  
**(b) Molded Thin Film Tray.** (Source: <https://www.impact-mfg.com>)

The challenge in designing the molded foam is that when it is holding objects with complex shapes, it is relatively difficult to create those undercut free cuts such that there is no interference between molded foam to the products during packing and unpacking processes. This is a tedious design process if designer decided to do it manually. Thus, chapter 3 introduces an efficient algorithm to automatically generate supporting surface to hold given products. It takes a commonly used file format, STL format, describing 3D models as the input and generates a smooth undercut-free supporting surface. The resultant model can be used to create molds for expended foams. The details of the algorithms and the methods used to reduce computational costs are presented and a number of examples are used to demonstrate the efficiency of the algorithm in the end of chapter 3.

In chapter 4, molded pulp is studied, an automated method of obtaining design space, and calculating locations for reinforcements is developed. A typical molded pulp structure for packaging consumer products is shown in Figure 1-5.



*Figure 1-5: A Typical Molded Pulp Packaging as a Tray to Hold Products in Position.*  
(Source: <http://www.pacificpulp.com>)

The supporting surface obtained in chapter 3 is used as reference to generate a thin layer topology design space for designing molded pulp. The topology optimization method described in chapter 2 is then applied to the design space; after the boundary conditions are specified; to find locations requires reinforcement on the thin-walled structure. Methods of converting the supporting surface into a 3D thin-walled design space and applying topology optimization to the space are presented and a number of examples are studied and the results are also shown in that chapter.

Finally in chapter 5, the main achievements of this research are briefly summarized and further extensions of the work are proposed.



## **Chapter 2.**

### **Design of Core Structures of Sandwich Board**

#### **2.1 Introduction**

In the mid 19<sup>th</sup> century, an ingenious concept enabled flimsy sheets of paper to be transformed into a rigid, stackable and cushioning form of packaging for delicate goods in transit. It is called corrugated board, cardboard, or sandwich board structure. Corrugated (also called pleated) paper was patented in England in 1856, but corrugated boxboard would not be patented and used as a shipping material until December 20, 1871. The patent was issued to Albert Jones of New York, New York for single-sided (single-face) corrugated board. Jones used the corrugated board for wrapping bottles and glass lantern chimneys. The first machine for producing large quantities of corrugated board was built in 1874 by G. Smyth, and in the same year Oliver Long improved upon Jones' design by inventing corrugated board with liner sheets on both sides. This was now corrugated board as we know it today.

An American Robert Gair invented the corrugated box in 1890, consisting of pre-cut flat pieces manufactured in bulk that folded into boxes. By the start of the 20th century, corrugated boxes began replacing the custom-made wooden crates and boxes previously used for trade. The corrugated carton was initially used for packaging glass and pottery containers, which are easily broken in transit. Later, the case enabled fruit and produce

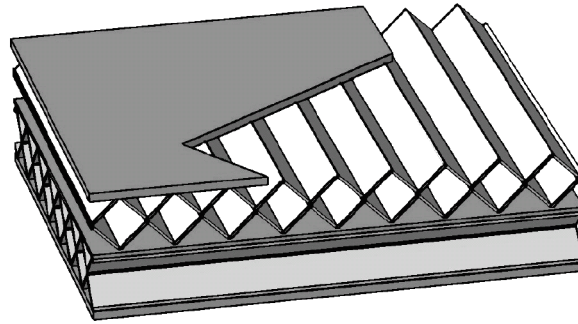
to be brought from the farm to the retailer without bruising, improving the return to the producers and opening up hitherto unaffordable export markets.

Today's corrugated board usually consists of outer flat sheets (liners) of puncture resistant paper, sandwiching a central "filling" of corrugated short fiber paper (fluted paper, core structure, or "medium"), which resists crushing under compression and gives cushioning protection to the box's contents. The outer and inner portions of the final corrugated board product are glued together along the outsides of the peaks and valleys of each flute, normally using starch adhesives. The starch is derived from corn, wheat or potato. Thus the complete make-up of corrugated board is from natural, sustainable materials in plentiful supply and the board is fully recyclable and can be pulped down to make more paper for more board once it has ended its own life.

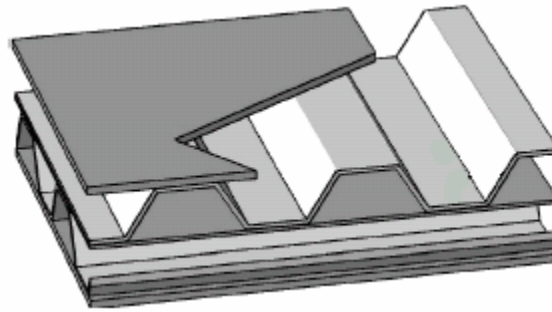
Old corrugated cartons are an excellent source of fiber for recycling. They can be compressed and baled for cost effective transport to anywhere in need of fiber for papermaking. Thus they help developing countries without sustainable wood resources build a paper and packaging industry locally and develop their exports to global markets. Today paperboard packaging in general, and especially products from certified sustainable sources, are receiving new attention, as manufacturers dealing with environmental, health, and regulatory issues look to renewable resources to meet increasing demand. It is now mandatory in many countries for paper-based packaging to be manufactured wholly or partially composed of recycled as well as tree-free fibers.

However, the core structure of the cardboard basically remains unchanged since its invention. Some researchers used some commonly seen structures or developed some

structures that can be easily fabricated to improve the sandwich structure. [21] Some examples of those core structures are illustrated in Figure 2-1.



(a)



(b)

*Figure 2-1: Some Commonly Seen Core Structures of Cardboard. [21]  
(a) Cross Corrugation. (b) Trapezoidal Corrugation.*

Some studies tried to develop parametric scheme on optimizing the core structures under different boundary conditions based on known stress pattern. This approach is similar to applying shape optimization from known topology. There is very little research on sandwich structures based on topology optimization approach to date. Topology optimization method, which is a sub-domain of structural optimization, does not limit the type of shapes in the design domain and tries to find a stiffest structure.

Structure optimization is an important problem in engineering. In practical engineering problems, engineers are always required to find a best design under certain target specifications and/or resource limitations that also satisfy some safety requirements and minimize the engineering cost at the same time. In order to fulfill the specifications, engineers may compose designs based on their background knowledge, intuition, experience, and by referencing some existing designs. The final design results usually differ from one designer to another. Thus, this intensive work may not guarantee to deliver the best design for the given constraints. The development of structural optimization methods provides a useful tool to engineers for searching the optimal design based on the given constraints in a timely manner.

Structural optimization methods can be categorized into two sets: Shape Optimization and Topology Optimization. They solve the basic engineering problem of distributing a limited amount of material in a design space.

Modern Topology optimization methods are based on finite element analysis (FEM), sensitivity analysis, optimization methods, linear algebra, and computer technologies. These methods utilize each finite element in the mesh for finite element analysis to be the design variables; obtain gradients of the objective function to the optimization problem formulation; and then update the variables to improve the current design toward the optimal one.

The fundamental concepts of topology optimization used in this study are introduced in the following sections. It includes problem formulation, material model, sensitivity analysis, and optimization algorithm.

## 2.2 Problem Formulation

The objective of topology optimization methods is to find a solid domain  $\Omega_s$ , which has limited volume  $\bar{V}$  included in a given domain  $\Omega$ , which maximizes or minimizes an objective function  $f$  while satisfying other constraints. A scheme of design domain is shown in Figure 2-2, where  $F_t$  is the external force and  $\Omega_v$  is a sub-domain without material.

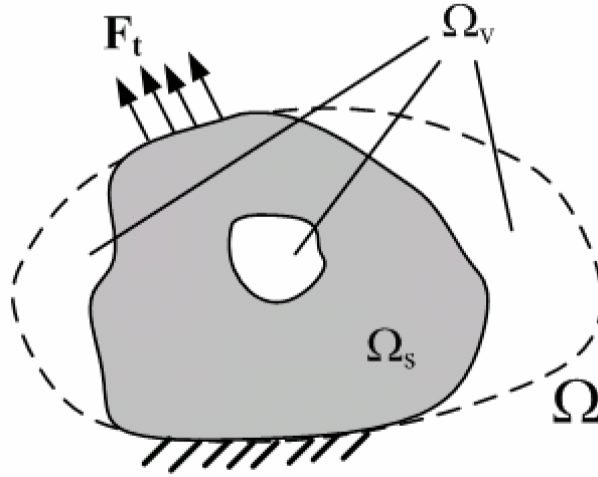


*Figure 2-2: Design Domain of Typical Topology Optimization Problem.*

The topology optimization problem is formulated to minimize or maximize an objection function, such as minimum mean compliance, and is usually formulated to have the form:

$$\begin{aligned} \min_{\rho} \left( \text{or } \max_{\rho} \right) \quad & f(\rho) \\ \text{s.t.} \quad & \int_{\Omega} \rho dv \leq \bar{V} \\ & \rho(v) = 0 \text{ or } 1, \quad \forall v \in \Omega, \end{aligned} \quad (2.1)$$

Where  $f(\rho)$  is the objective function,  $\bar{V}$  is the upper bound of the solid volume, and  $\rho$  is density distribution in domain  $\Omega$  which is 1 in subdomain  $\Omega_s$ , 0 in subdomain  $\Omega_v$ .

However, there is no direct method that can solve this optimization problem efficiently over the solid continuum. Thus, methods of discretizing the design domain  $\Omega$  into a number of finite elements are generally used for topology optimization problems. Each finite element is assigned as a design variable  $\rho_i$  which represents the density of the element. Therefore, a vector  $\rho$  consisting of all design variables are used to represent the density distribution in the design domain in order to solve the topology optimization problem. As a result, the discretized topology optimization problem formulation is represented as the form:

$$\begin{aligned} \min_{\rho} \left( \text{or } \max_{\rho} \right) \quad & f(\rho) \\ \text{s.t.} \quad & \sum_i^N \rho_i v_i \leq \bar{V} \\ & \rho_i = 0 \text{ or } 1, \quad i = 1, \dots, N, \end{aligned} \quad (2.2)$$

where  $v_i$  is the volume of the  $i^{\text{th}}$  element.

Some studies indicated that this binary topology optimization problem formulated in Equation (2.2) lacks of solutions [22]. There are some numerical instabilities found in the numerical solutions to the problem such as the checkerboard effect and mesh-dependency. These instabilities can not be eliminated by refining the finite element mesh. Previous studies suggested a few methods to overcome these problems, such as restriction methods and relaxation methods. Restriction methods reduce the design set by introducing some extra constraints to avoid oscillation of  $\rho$ . For instance, Haber et al. [23] presented some results with an extra bound of the perimeter of the boundary between solid and void subdomain. Relaxation methods extend the design set to achieve existence of solutions. Fro instance, Bendsoe et al [24] introduced a

homogenization approach to topology optimization by using a perforated microstructure before computing the effective material properties which makes the material density varies from 0 to 1.

In this study, relaxation methods are used to model and solve topology optimization problems for packaging applications. The material model is presented in the next section.

## **2.3 Microstructure Based Composite Material Models**

As aforementioned, the instabilities of the binary topology optimization problem are difficult to solve. It can be overcome by allowing the design variables, the element volume density, to vary from 0 to 1. For the elements with volume density between 0 and 1, they can be treated as new composite materials which have a different microstructure in it. In order to properly treat the element stiffness, a material model needs to be determined and applied during finite element analysis. Many material models have been introduced to structural topology optimization problems in the past decades. Some well-known models are the Hole-in-cell microstructure model presented by Bendsoe and Kikuchi [24] in 1988; the Solid Isotropic Microstructure with Penalty (SIMP) presented by Bendsoe [25] in 1989; and the Spherical Micro-inclusion model presented by Gea [26] in 1996. Among these models, SIMP is simple and commonly used in this field; and Micro-inclusion models can be used in the topology optimization problem with a multi-material substance. They are discussed and compared in the following section.

### 2.3.1 Solid Isotropic Microstructure with Penalty Model

Bendsoe [25] introduced a material model, Solid Isotropic Microstructure with Penalty (SIMP), in 1989 to simplify topology optimization and finite element analysis procedures.

In the SIMP model, the elastic tensor  $E_{ijkl}$  of a given solid isotropic reference material and the volume  $V$  of material in the design space is defined as:

$$E_{ijkl}(x) = \rho(x)^p E_{ijkl}^0, \quad p > 1 \quad (2.3)$$

$$V = \int_{\Omega} \rho(x) d\Omega \quad (2.4)$$

where  $\Omega$  is the design domain;  $x$  is the design variable of each finite element and  $x \in \Omega$ ;  $\rho(x)$  is the volume density of each element and  $0 \leq \rho(x) \leq 1$ ;  $p$  is a penalty coefficient to the material, which is greater than 1 to provide penalty on stiffness of the material considering the volume density  $\rho(x)$  is between 0 and 1, as stated in equation (2.3). The effect of different penalty values  $p$  to the relative stiffness  $(E/E^0)$  is illustrated in Figure 2-3.

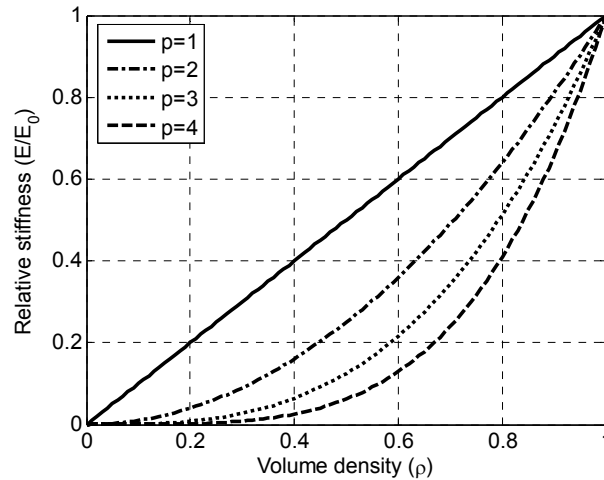
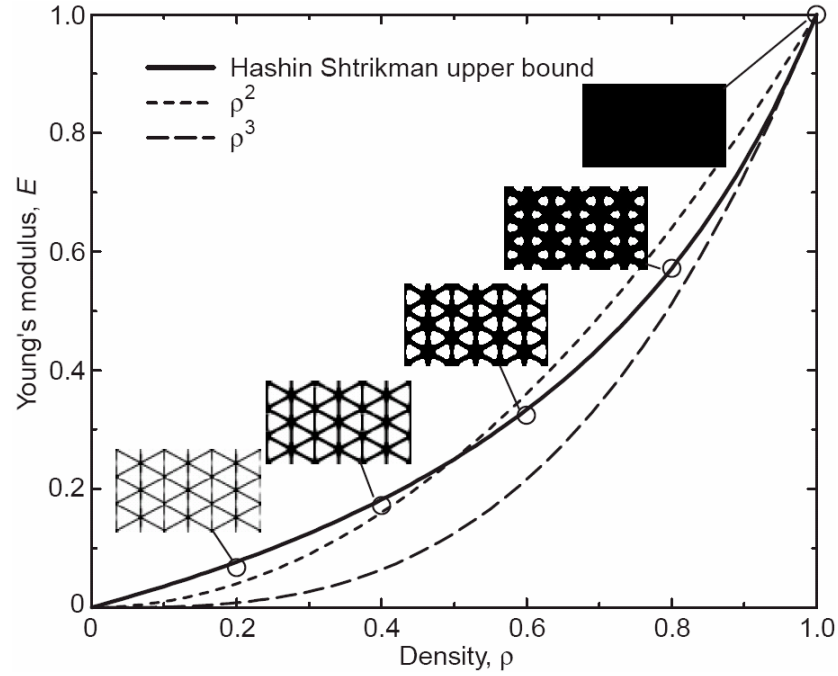


Figure 2-3: Penalization of the Intermediate Volume Densities in SIMP Model [25].



It is clear, as shown in Figure 2-3, that when the penalty power  $p$  increases, the curve has a tendency to become a step function. Therefore, using void ( $\rho = 0$ ) or solid ( $\rho = 1$ ) in the topology optimization design will be more effective than using intermediate density values in the SIMP model. Hence, the result of topology optimization will tend to generate an optimal design with mostly solid and void phase and avoid phases with intermediate density values. The result fits the expectation result desired in the formulation stated in equation (2.2).

Although the SIMP model provides expected condensed topology results, it had been always called artificial or a fictitious material model since there is no physical interpolation to the region with intermediate density values. In 1999, Bendsoe and Sigmund [27] compared some material models such as variable thickness bound, the Hashin-Shtrikman bound, as well as the SIMP model. A comparison between the SIMP model and the Hashin-Shtrikman upper bound for an isotropic material can be seen in Figure 2-4. The Microstructures of material and void realizing the material properties of the SIMP model can be found in Figure 2-5.



**Figure 2-4: A Comparison of the SIMP Model and the Hashin-Shtrikman Upper Bound for an Isotropic Material With Poisson Ratio  $\nu = 1/3$  mixed with void. For the H-S Upper Bound, Microstructures With Properties Almost Attaining the Bounds Are Also Shown. [27]**

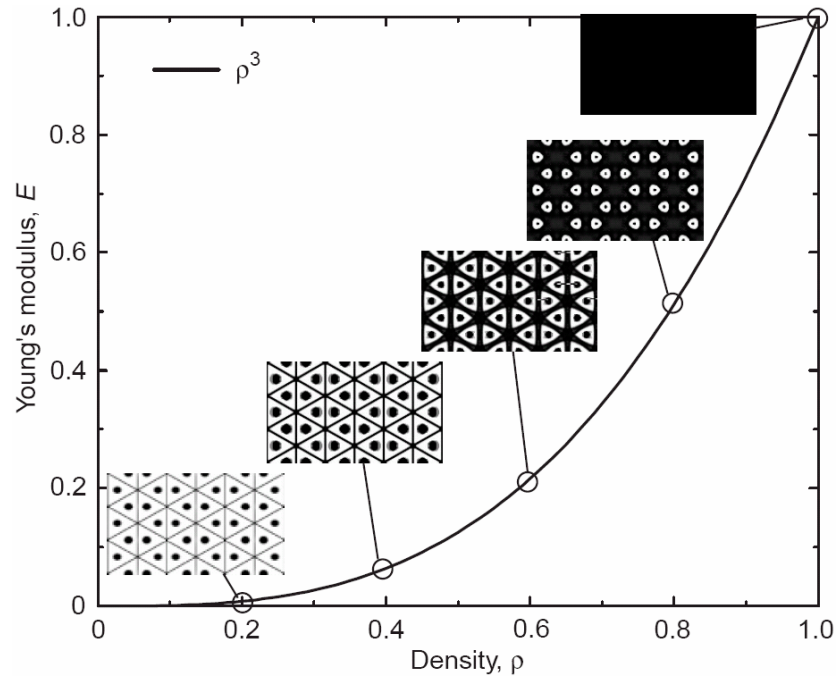


**Figure 2-5: Microstructures of Material and Void Realizing the Material Properties of the SIMP Model With  $p = 3$ , for a Base material With Poisson's Ratio  $\nu = 1/3$ . As Stiffer Material Microstructures Can Be Constructed From the Given Densities, Non-structural Areas Are Seen at the Cell Centers. [27]**

As the microstructures are constructed from a given density and penalty values, the use of the term “density” for the variable  $\rho$  is quite natural for the SIMP material model.

### 2.3.2 Spherical Micro-inclusion Model

The homogenization methods strictly formulate the relation between the elastic tensor and the volume density of a unit cell with periodic microstructures. The SIMP model provides a relatively simple approach to solve the topology optimization problem. However, it is not usually obvious to select an appropriate penalty power  $p$  for a particular material. Some research used different values of  $p$  and the justification is not persuasive. In 1996, Gea [28] proposed another microstructure-based material model, the spherical micro-inclusion model, which not only has a rigorous formulation but is also easy to use.

An illustration of the micro-inclusion material model is shown in Figure 2-6. An infinite number of isotropic spherical voids are embedded in an isotropic base material in an element. For this composite material model, the material properties are derived by means of Mori-Tanaka’s mean field theory in conjunction with Eshelby’s equivalence principle and his solution of an ellipsoidal inclusion.

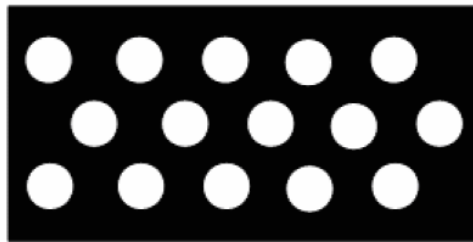


*Figure 2-6: Microstructure of the Spherical Micro-inclusion Material Model.[28]*

Assuming a base material with Poisson's ratio  $\nu_0 = 1/3$ , the effective Young's modulus and shear modulus are given by

$$E = \frac{c_0}{2 - c_0} E_0, \quad 0 \leq c_0 \leq 1 \quad (2.5)$$

and

$$\mu = \frac{8c_0}{15 - 7c_0} \mu_0, \quad 0 \leq c_0 \leq 1 \quad (2.6)$$

where  $c_0$  is the volume fraction of the base material in the element. The relation between the relative stiffness ( $E/E_0$ ) of the sphere micro-inclusion model and volume fraction  $c_0$  is shown in Figure 2-7. For comparison, the SIMP model with penalization power  $p = 2$  is shown as the dashed curve. It is clear that they are fairly close to each other.

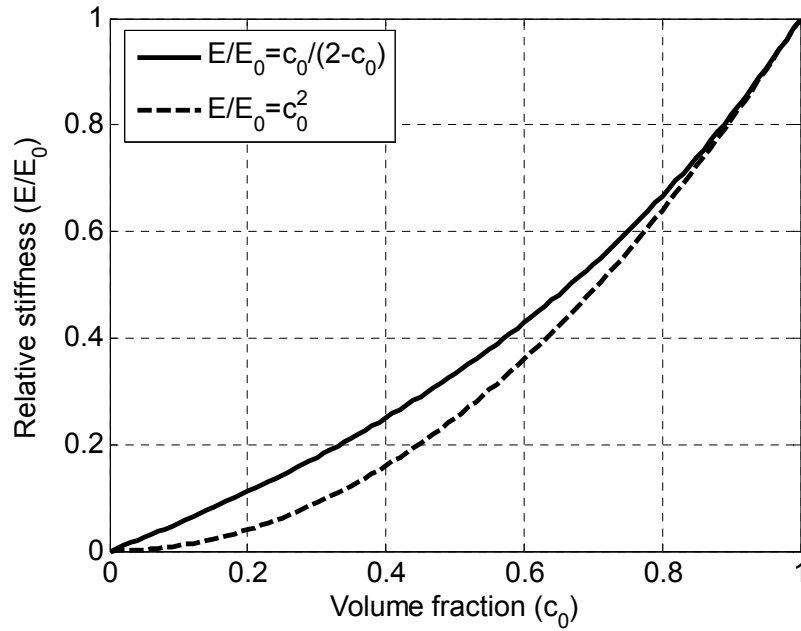


**Figure 2-7: Relative Stiffness vs. Volume Fraction for the Spherical Micro-inclusion Model and the SIMP Model With Penalization Power  $p = 2$ .**

It is worth noticing that the spherical micro-inclusion material model could be easily extended to the multi-material model [29], similar to the SIMP model [27].

## 2.4 Optimization Algorithm Using Optimality Criteria

As aforementioned in the problem formulation section, the topology optimization problem is formulated as in equation (2.2). Consider a topology optimization problem for minimizing the total mean compliance, which is defined as twice of total strain energy, of a structure stated as following:

$$\begin{aligned}
 \min_x \quad & \Pi(X) = U^T K U \\
 s.t. \quad & V(X) = \sum_{i=0}^N x_i v_i \leq \bar{V}_0 \\
 & KU = F \\
 & X = \{x_1, x_2, \dots, x_N\}, \quad \underline{x} \leq x_i \leq \bar{x}
 \end{aligned} \tag{2.7}$$

where  $N$  is the number of design variables, and  $v_i$  is the volume of an element.  $KU = F$  is the equilibrium equation where  $K$  denotes the stiffness matrix,  $F$  denotes the loading vector to the structure and  $U$  denotes the displacement field. Consider the current design point is located at point  $X^k$ , a local linear approximation is applied to the objective function using the first order Taylor expansion:

$$\begin{aligned}
 \min_x \quad & \Pi(X) = \Pi_0 + \sum_{i=1}^N \frac{\partial \Pi_i}{\partial x_i} (x_i - x_i^k) \\
 s.t. \quad & V(X) = \sum_{i=0}^N x_i v_i \leq \bar{V}_0 \\
 & X = \{x_1, x_2, \dots, x_N\}, \quad \underline{x}^k \leq x_i \leq \bar{x}^k
 \end{aligned} \tag{2.8}$$

Consider a variable offsetting  $y_i = x_i - \underline{x}$  while collecting constant terms to a bulk constant for current strain energy and adjusted volume, and replace derivatives of variables. Then equation (2.8) can be rewrite as follows:

$$\begin{aligned} \min_y \quad & \Pi(Y) = \Pi_1 + \sum_{i=1}^N \frac{\partial \Pi_i}{\partial y_i} y_i \\ \text{s.t.} \quad & V(Y) = \sum_{i=0}^N y_i v_i \leq \bar{V}_1 \\ & Y = \{y_1, y_2, \dots, y_N\}, \quad 0 \leq y_i \leq \bar{y}^k \end{aligned} \quad (2.9)$$

Furthermore, apply a variable scaling to variable  $Y$ , defined as  $z_i = y_i v_i$  and its derivative  $dz_i = v_i dy_i$ , where  $v_i$  is the volume of the  $i^{\text{th}}$  element. Equation (2.9) can be further written as:

$$\begin{aligned} \min_z \quad & \Pi(Z) = \Pi_1 + \sum_{i=1}^N \frac{\partial \Pi_i}{\partial z_i} z_i \\ \text{s.t.} \quad & V(Z) = \sum_{i=0}^N z_i \leq \bar{V}_1 \\ & Z = \{z_1, z_2, \dots, z_N\}, \quad 0 \leq z_i \leq \bar{z}^k \end{aligned} \quad (2.10)$$

Notice that by applying the variable transformations back to the sensitivity term in equation (2.10), the following equation can be obtained:

$$\begin{aligned} y_i = x_i - \underline{x} &\Rightarrow dy_i = dx_i, \quad z_i = v_i y_i \Rightarrow dz_i = v_i dy_i \\ \frac{d\Pi_i}{dz_i} &= \frac{\partial \Pi_i}{\partial y_i} \frac{dy_i}{dz_i} = \frac{\partial \Pi_i}{\partial x_i} \frac{dy_i}{dz_i} = \frac{\partial \Pi_i}{\partial x_i} \frac{1}{v_i} = \frac{\partial (\Pi_i / v_i)}{\partial x_i} \end{aligned} \quad (2.11)$$

The physical meaning of the sensitivity term stated in equation (2.11) and equation (2.10) is that the order of updating the design variable is based on the sensitivity of energy density of each element. This formulation can eliminate the distortion effect of the topology when the element size is not uniform. The distortion effect is that when a design space with non-uniform element sizes is used and when the sensitivity of total energy in

each element is considered as the weight of its density in traditional formulation, the element with larger volume always get higher density than it should be. In this formulation the sensitivity of energy density is considered such that the distortion effect is minimized.

Equation (2.10) is a simple linear programming (LP) form where all the constraints have their coefficients as positive values. It requires a basic solution to start with and by trading variables values, it can reach an optimal. The order of the trading scheme depends on the coefficients of design variables,  $\partial\Pi/\partial z_i$ , in the objective function.

The calculation of  $\partial\Pi/\partial z_i$  is called sensitivity analysis which provides gradients of the objection function with respect to variables. The calculation of design sensitivity analysis can be performed by two different approaches [30]: the variational approach and the discretized approach. The variational approach is to apply the variational principle to differentiate the governing equations before they are discretized, and then solve the resulting equations by structural analysis programs. The discretized approach uses finite element models to carry out the analysis. The sensitivity calculation is then equivalent to determining the derivatives of a given function. The discretized approach for sensitivity analysis has three different computational schemes: the analytical method, the semi-analytical method, the finite differencing approximation. The analytical method of the discretized approach is used here because of its computational advantages.

The sensitivity of the total strain energy  $\partial\Pi/\partial z_i$ , defined in equation (2.10), can be obtained by applying the chain rule of differentiation as follows:

$$\frac{d\Pi}{dz} = \frac{\partial\Pi}{\partial y} \frac{dy}{dz} = \frac{\partial}{\partial y} \left( U^T K U \right) \frac{1}{v} = \left( 2U^T K \frac{\partial U}{\partial y} + U^T \frac{\partial K}{\partial y} U \right) \frac{1}{v} \quad (2.12)$$

The item  $\partial U/\partial y$  on the right hand side of equation (2.12) can be obtained by differentiating the equilibrium equation  $KU = F$  with respect to the design variable  $y$ :

$$K \frac{\partial U}{\partial y} + \frac{\partial K}{\partial y} U = \frac{\partial F}{\partial y}. \quad (2.13)$$

and can be rearranged into:

$$\frac{dU}{dy} = K^{-1} \left( -\frac{\partial K}{\partial y} U + \frac{\partial F}{\partial y} \right). \quad (2.14)$$

Combine equation (2.12) and (2.14) into one equation, which has the form:

$$\begin{aligned} \frac{d\Pi}{dz} &= \left( 2U^T K K^{-1} \left( -\frac{\partial K}{\partial y} U + \frac{\partial F}{\partial y} \right) + U^T \frac{\partial K}{\partial y} U \right) \frac{1}{v} \\ &= \left( -U^T \frac{\partial K}{\partial y} U + \frac{\partial F}{\partial y} \right) \frac{1}{v} \end{aligned} \quad (2.15)$$

The global stiffness matrix is assembled from individual stiffness matrices at the element level. Therefore,  $K$  is a function of the element density only. Assume the material strength is a function of design variable which can be defined as follows:

$$k_i = f(y_i) k_0^e \quad (2.16)$$

where  $k_0^e$  is the stiffness matrix with full material. Then consider  $F$  is a constant, then the sensitivity becomes:



$$\begin{aligned}
\frac{d\Pi^e}{dz_i} &= \left( -u_i^T \frac{\partial k_i}{\partial y_i} u_i \right) \frac{1}{v_i} \\
&= \left( -\frac{df(y_i)}{dy_i} u_i^T k_0^e u_i \right) \frac{1}{v_i} \\
&= -\left( \frac{df(y_i)/dy_i}{f(y_i)} u_i^T f(y_i) k_0^e u_i \right) \frac{1}{v_i} \\
&= -\left( \frac{df(y_i)/dy_i}{f(y_i)} u_i^T k_i u_i \right) \frac{1}{v_i} \\
&= -\frac{f'_i}{f_i} \frac{\Pi_i^e}{v_i}.
\end{aligned} \tag{2.17}$$

Substitute the sensitivity term back into equation (2.10), the optimization problem can be reorganize as follows:

$$\begin{aligned}
\min_z \quad & \Pi(Z) = \Pi_1 - \sum_{i=1}^N \frac{f'_i}{f_i} \frac{\Pi_i^e}{v_i} z_i \\
s.t. \quad & V(Z) = \sum_{i=0}^N z_i \leq \bar{V}_1 \\
& Z = \{z_1, z_2, \dots, z_N\}, \quad 0 \leq z_i \leq \bar{z}^k
\end{aligned} \tag{2.18}$$

which can be easily solved.

In equation (2.18), the sensitivities of energy density of each element can be considered as the coefficients of the design variables in the objection function, thus, the higher the

term  $\frac{f'_i}{f_i} \frac{\Pi_i^e}{v_i}$  is, the design variable should be increased first, and vise versa. Since the

displacement field  $U$  is obtained from finite element analysis, it is simple to calculate these sensitivities. Hence, a simple sorting of the sensitivity can greatly simplify the updating process.

The other issue to notice is that the sensitivity analysis linearizes the objective function in an infinitely small area around the current design point. Thus the perturbation of design

variables should be kept small. Typical perturbation of design variables is five percent of the volume density. This value contracts when the objective function stops descending or starts oscillating.

To demonstrate the feasibility of this method, a number of examples are presented and discussed in the following section.

## **2.5 Examples**

In this section, results of two examples obtained by the optimization method aforementioned are presented and discussed. The first example is a typical topology optimization problem: a short cantilever beam. The second example is a 3D cantilever beam. These two examples demonstrate that the topology optimization method discussed in this chapter works on both 2D and 3D cases.

### **2.5.1 Example 1: A Short Cantilever Beam**

Consider a short cantilever beam subjected to a vertical load at the middle of the right side and its entire left side is clamped. As shown in Figure 2-8. The design objective is to minimize the mean compliance while satisfying a maximum volume constraint; in this example the volume constraint is set to be 30 percent of the total design domain. This problem is a well-known topology optimization problem and the result has been reported in many articles. The optimal topology obtained from this study is shown in Figure 2-9 and is very close to the ones reported but without those tiny structures that are difficult to fabricate.

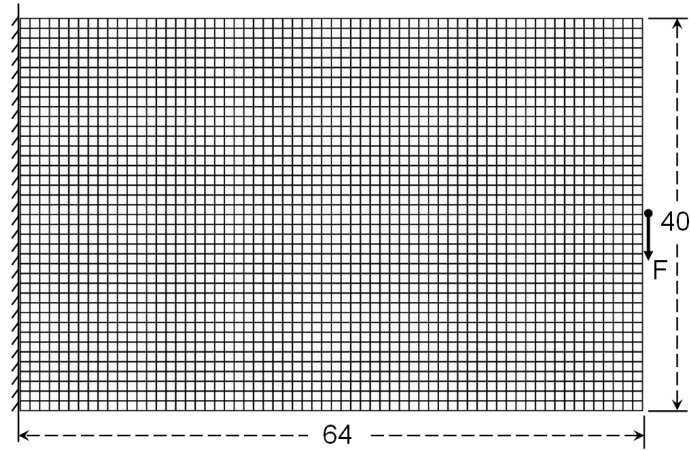


*Figure 2-8: A Short Cantilever Beam Is Subjected to a Vertical Load in the Middle of the Right Side and Clamped on the Left Side.*

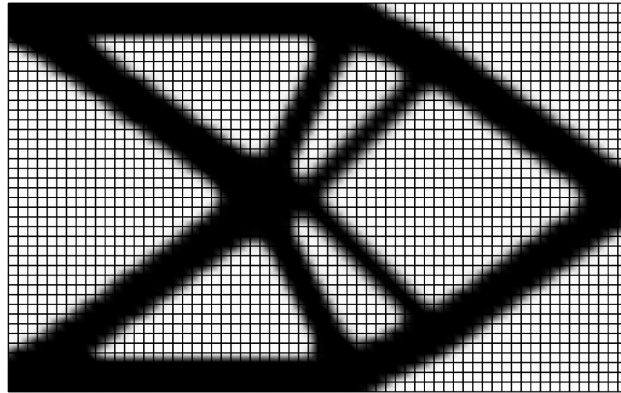


*Figure 2-9: The Result of the Short Cantilever Beam Subject to the Boundary Conditions Shown in Figure 2-8.*

### 2.5.2 Example 2: A 3D Cantilever Beam

The final example is to exemplify the ability of this method to 3D topology designs. A 3D cantilever beam subjected to a vertical load at the middle of the lower right edge and the four corners of the left side are fixed. The design domain is shown in Figure 2-10. The design objective is also to find a stiffest structure with a volume constraint set to 20%. The result is shown in Figure 2-11 and Figure 2-12.

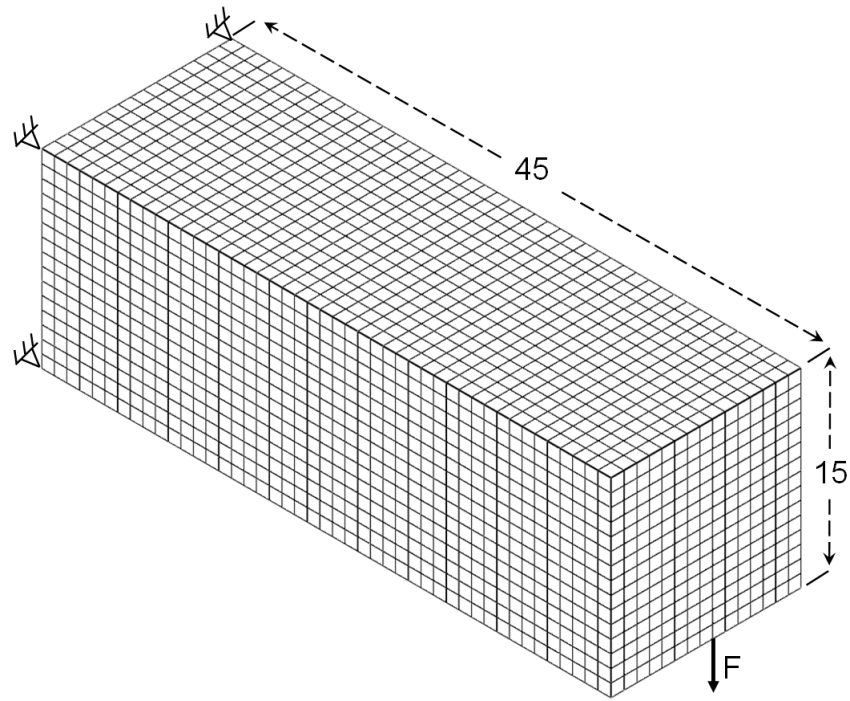


*Figure 2-10: A 3D Cantilever Beam Is Subjected to a Vertical Load at the Center of its Right Bottom Edge with its Four Left Corners Fixed.*

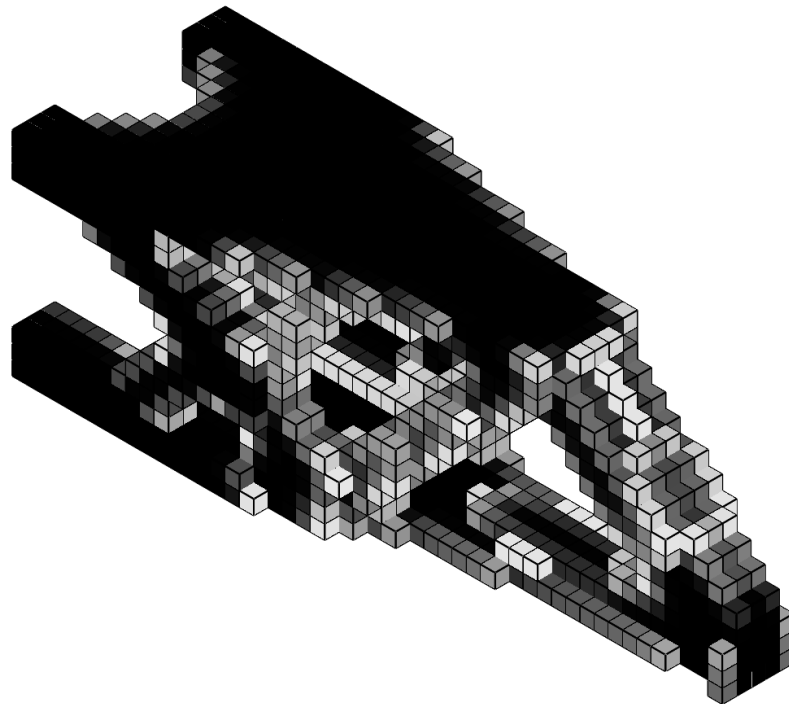


*Figure 2-11: The Optimal Topology of the 3D Cantilever With the Boundary Conditions Shown in Figure 2-10.*

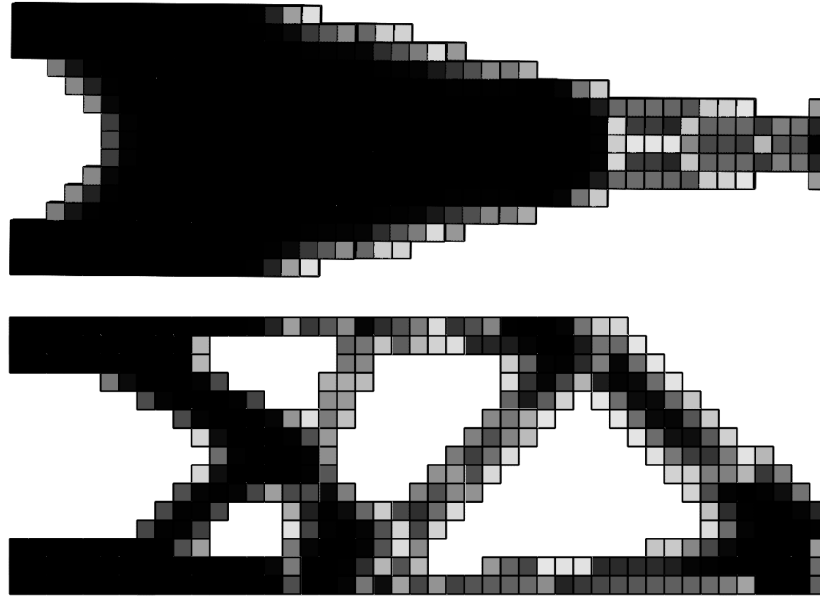


*Figure 2-12: Top View and Front view of the Same Result Shown in Figure 2-11.*

## 2.6 Optimization of Core Structure of Sandwich Board

The topology optimization process discussed in this chapter is used to design the stiffest sandwich structure that can be visualized as cardboard which is commonly used for boxing in the packaging industry. As studied of the strength of the sandwich core structure in other research, the sandwich structure is considered as a cantilever beam with one end clamped under a vertical load [5-7, 31]. Actual test setup is similar to the one shown in Figure 2-13. Three design spaces are considered as: (1) a unit sandwich cell under bending load, (2) two sandwich cells under different loads, and (3) a long sandwich beam under bending load. Symmetric constraints are used in these designs since the structure is considered as a recurrent structure. The details of the modeling process and results are discussed in the following section.

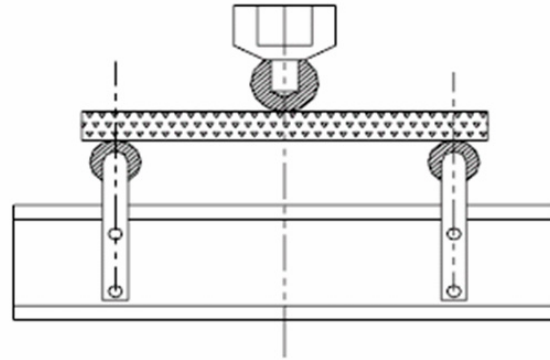


*Figure 2-13: Sandwich Board Strength Test Setup.*  
(Source: Industrial and System Engineering Dept. at Rutgers Univ.)

### 2.6.1 Design 1: A Single Cell Sandwich Structure

The first example considers the design space as a single cell of the sandwich board subject to bending load with the design space divided into  $40 \times 40$  elements. According to the test setup shown in Figure 2-14, the lower left corner of the design space is allowed to roll along horizontal direction. The right edge is simple supported that allows rolling along vertical direction. A vertical force pointing down is placed at the upper right corner. The upper and lower layers are defined to have non-designable density as 1 to represent to plates of the sandwich structure. The volume constraint is set up to 10 percent of the total volume. The design spaces and the optimized result can be found in Figure 2-14.

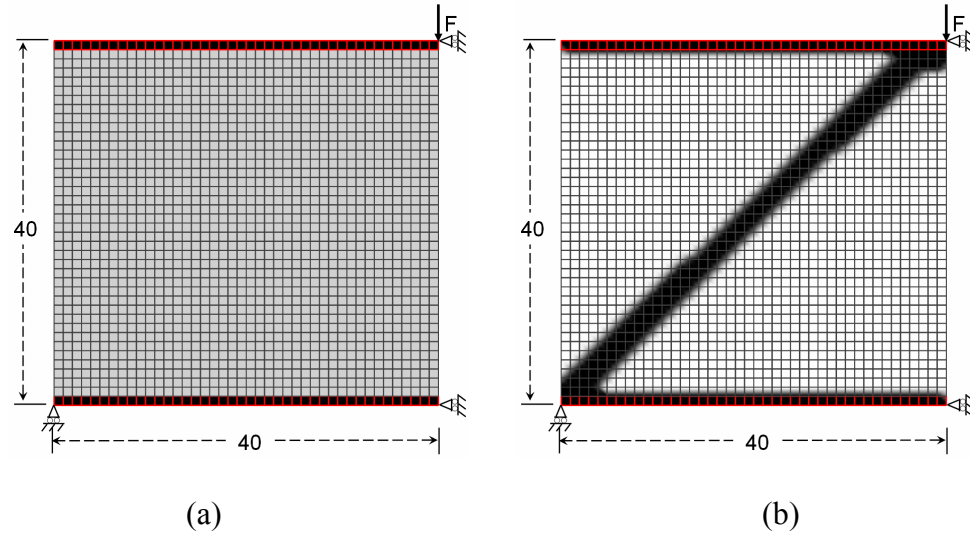


**Figure 2-14: (a) Single Cell Design Space of a Sandwich Board. Left is fixed while right is rolling. A force is placed at the upper right corner. The volume constraint is 10 percent (b) Topology Optimization Result.**

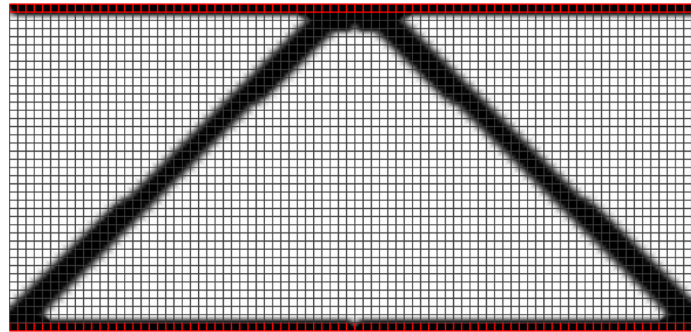


**Figure 2-15: Mirrored Topology Optimization Result of the Single Cell Design to Show the Whole Design.**

In order to verify this triangular structure is not a trivial solution to the boundary conditions and constraints, a double cell design space is examined and is presented in the next example.

## 2.6.2 Design 2: A Multiple Cell Sandwich Structure

A design space is formed to have an aspect ratio of 3 for mimicking a double cell design space. The design space is composed to have 120 x 40 elements. The boundary conditions are defined similar to the previous design. The upper and lower layers are

defined to have density as 1 and set the volume constraint to 10 percent. Symmetric constraints are placed in order to simulate periodic structures. The design space and result are illustrated in Figure 2-17.

This design also shows triangular structures as the sandwich core. These results indicate that the triangular structure is the stiffest structure for sandwich board and it repeats twice as expected when setup the design space for verification.

It is reasonable to assume that the triangular structure will repeat along long beam sandwich board structure. Thus, a long beam structure is composed to confirm this hypothesis. The long beam case is presented as the next example.

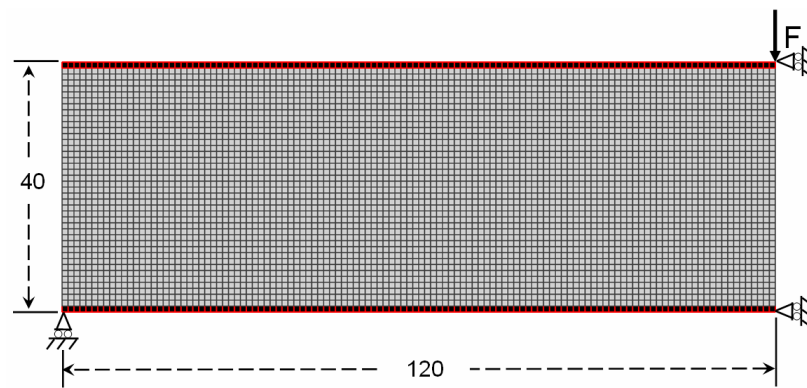


*Figure 2-16: Design Space of Multiple Cell Sandwich Structure.*

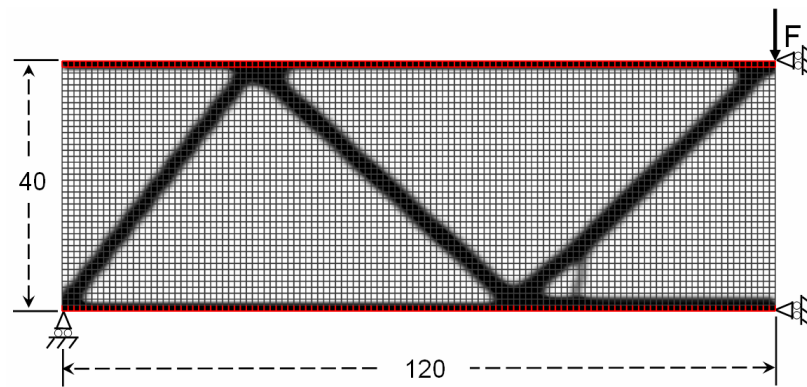


*Figure 2-17: Topology Optimization Result. Upper and lower layers are set to be non-designable with densities to be 0.3 and the volume constraint is 10 percent.*



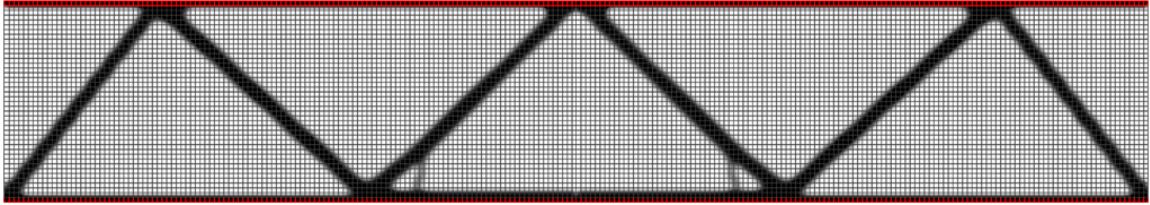


*Figure 2-18: Mirrored Topology Optimization Result of Multiple Cell Design to Show the Whole Design.*

### **2.6.3 Design 3: A Thin and Long Sandwich Beam**

A long beam with a design space consisting of  $200 \times 20$  elements is composed and solved to find the best core structure in the sandwich board. The lower left corner is simply supported along horizontal direction when the right edge is allowed to roll along vertical direction. A vertical load is placed at the upper right corner. The densities of elements in upper and lower layer are setup to 1 and are non designable. Detailed design space and boundary conditions are shown in Figure 2-21. The upper volume constraint is configured to 10 percent and the optimized result is shown in Figure 2-22. The result shows repeated triangular structures in the middle as the core structure of the sandwich board which, again, confirms the designs performed in the previous examples. This structure can be visualized by taking the structure and extruding out to form a 3D plate as shown in Figure 2-23. This plate uses two sandwich structures and stacks them up while arranging them in orthogonal orientation for better performance considering loads may be applied to the plate from other different directions.

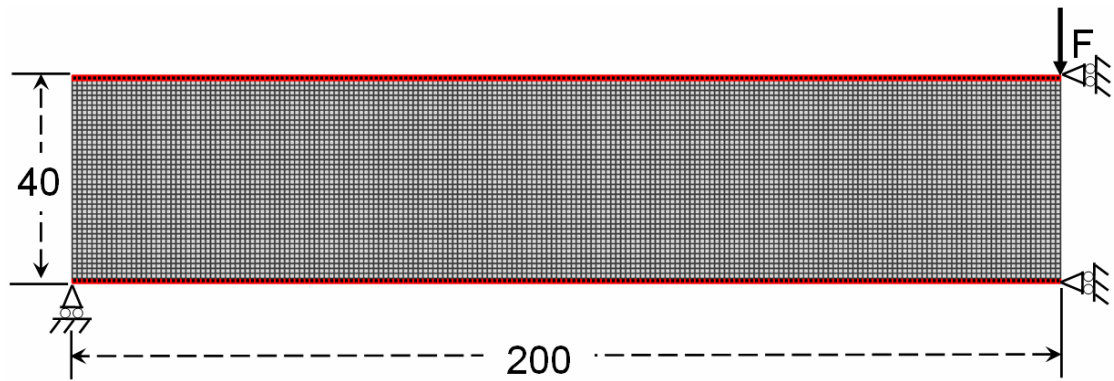


*Figure 2-19: Design space of a Long Sandwich Board Structure Divided into 200 x 40 Elements.*

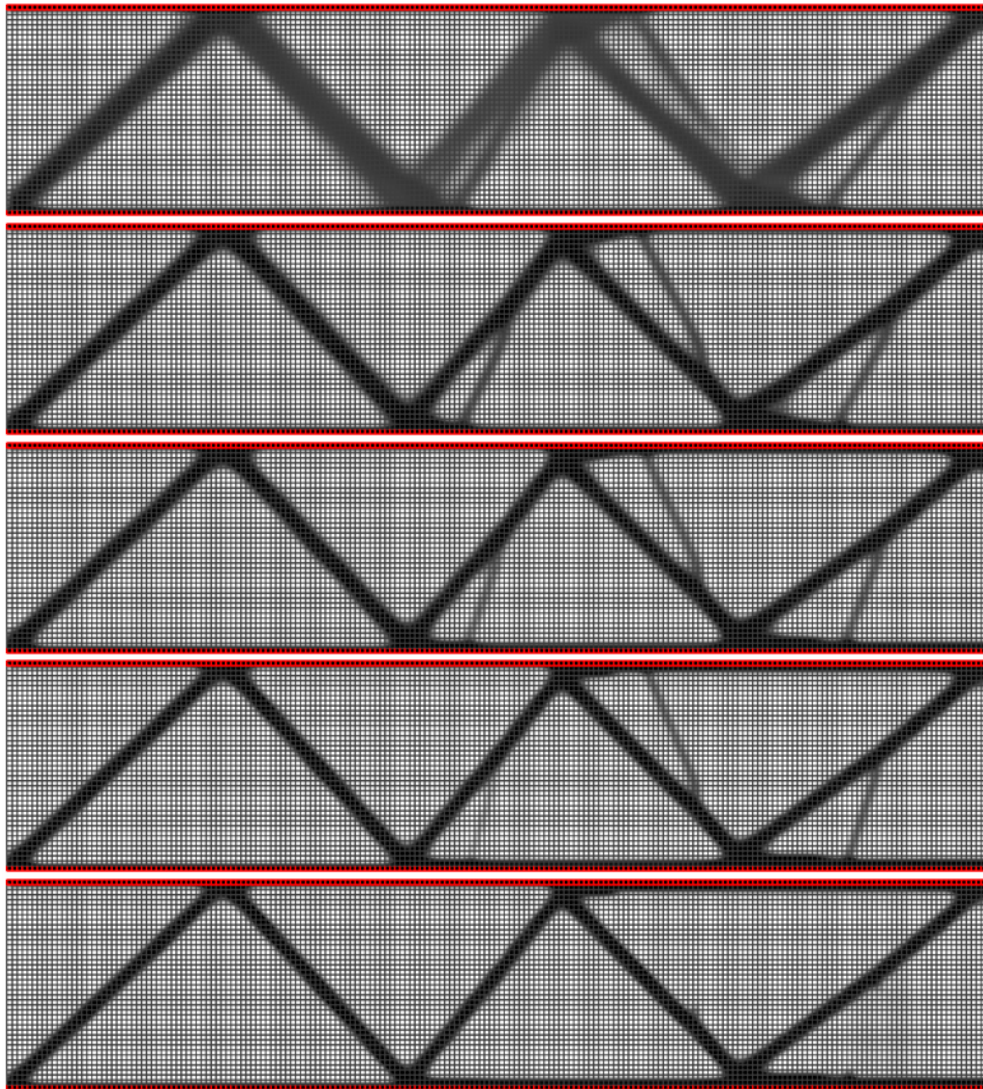


*Figure 2-20: Historiography Data of the Long Sandwich Board Design.*

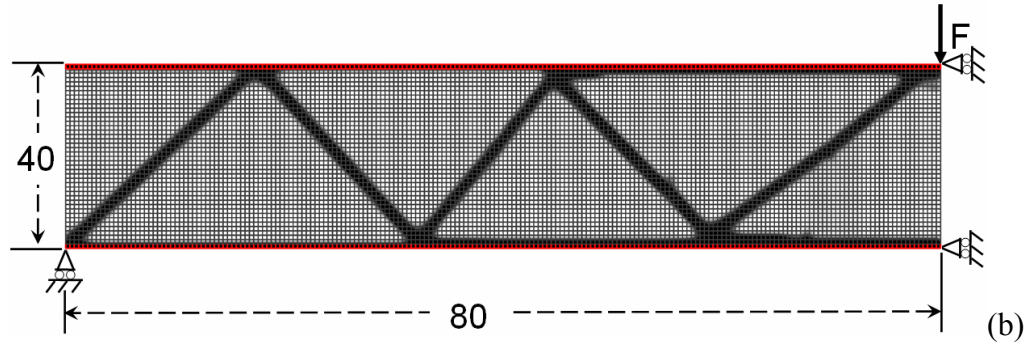


*Figure 2-21: Final Topology Optimization Result of the Long Sandwich Board.  
10 percent of the volume is specified to be the upper limit.*

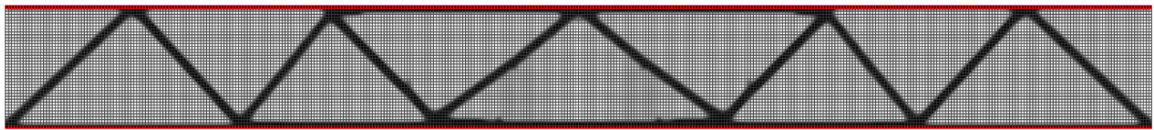


*Figure 2-22: Topology Optimization Result of Long Sandwich Design to Show the Whole Design.*

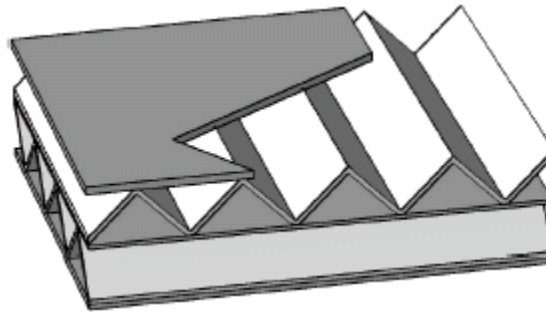


*Figure 2-23: 3D Visualization of the Sandwich Design Presented and Discussed in This Section. [21]*

The triangular core structure of a sandwich board is confirmed in another research by Carlessen in 2001 to have the maximum transverse shear modulus.[32]

## 2.7 Conclusion and Remarks

Application of the topology optimization method to the sandwich structure design is carried out and discussed in this chapter. This method provides consistent results

throughout different size of problems. The result is visualized to a double layer sandwich structure which is studied by other researcher and, having been studied by other researchers, has been proven to be stiff enough.

An efficient and yet simple topology optimization method, related analyses, and a few examples are discussed in this chapter. This topology optimization method discussed in this chapter constructed a simple design variable updating scheme that keeps all improved designs satisfying all necessary optimality conditions of the locally approximated problem. The results generated by this method provide similar results comparing to other studies. However, there are no undersized features in the resultant topology which make the result friendlier to post-processing, such as shape optimization and feature extraction, and to manufacturability.

The method discussed in this chapter provides proper results. It can be applied to some practical situations as long as the boundary conditions are well defined. Some practical examples will be discussed in the later chapters.



## **Chapter 3.**

### **Design of Packaging Supporting Tray**

#### **3.1 Introduction**

For industrial packaging, the fixed format method is commonly used because it provides better space efficiency and outstanding protection to the products than loose fit type of packaging. In order to package products with irregular shapes, the molded packaging supporting tray such as molded foam like Expanded Polystyrene (EPS) and thin plastic film tray are generally used to hold the product in a desired position along with all the accessories they may have. Typical examples of supporting trays are shown in Figure 3-1.

The supporting tray is designed so that all the products can be placed into the packaging space and the position of the products can be fixed to prevent collision and any damage that may come from transportation and stocking. The supporting tray should be stiff enough to resist stress hardening and is yet soft enough to absorb shocks and vibrations such that the products it is holding are well protected in a safe environment. The foam type of tray is usually used when products require outstanding shock absorption or thermal isolation. The thin film type of tray is generally used on lightweight consumer products especially when transparency is important for product demonstration.



(a)



(b)

**Figure 3-1: Examples of Supporting Tray.**  
(a) Polyurethane foam tray. (<http://www.gwwcases.com>)  
(b) Thin film plastic tray. (<http://www.arrowheadinc.com>)

The essential design of supporting tray is the supporting surface that contacts with products to provide support. The supporting surface should provide a space that products can be placed in and taken out without any difficulties or interference to the tray itself.

The design of molded supporting tray usually takes a few steps such as: (1) Convert the native CAD model format created in some CAD software packages to a neutral model format. (2) Arrange the product models including its accessories to a desired presentation or position and define the outer bounding box. (3) Design a supporting surface. (4) Export a manufacturable file format of the mold of the supporting tray as a bulk or as a thin film.

First, the packaging company receives orders for products to be packaged in the form of CAD models or physical products. The CAD models may be given in its native CAD formats or in their surface representation formats due to product confidentiality. The surface representation may be in B-spline representation format such as The Initial Graphics Exchange Specification (IGES) and Standard for the Exchange of Product Data (STEP); or in facet representation format like Stereo Lithography Format (STL). If physical models are provided, digitalization method of the products can be used to convert the products to digitalized 3D data for surface representation. In the manufacturing point of view, STL format is more commonly used in the manufacturing industry because it uses small triangles to describe a model and the triangle is one of the most basic primitives for computer graphics, and it is easy to be handled. Thus, in either way, STL data format is used to describe surface information.

The second procedure is to arrange the products in a bounding box. Normally, the arrangement of product, such as orientation, and the overall size packaged box can be pre-determined based on display requirements and/or weight distribution.

Followed by the main procedure of designing the mold to support / hold the products in the package. The mold can be exported to a file format that the manufacturer requires,

usually the STL format. Therefore, the task of the packaging company is to design the supporting space between the bounding box and the products. Traditional methods based on Boolean Operations can be used to create a negative image model for the packaging space between the bounding box and the products. Traditional mold creating techniques, such as Boolean Operations, Parting line detection [33-35], and injection mold generation methods [36, 37], can be used to generate supporting surface. Although these approaches are considerably straightforward for the convex model packaging, it may create a faulty design for concave shapes as shown in Figure 3-2. The Figure 3-2(a) indicates a supporting bulk generated using simple Boolean difference operation. It has the portion inside the cup model and the handle that is not possible to insert the cup into the bulk. The Figure 3-2(b) indicates a feasible design for the cup model that the cup can be placed into and remove from the bulk without any difficulties. To overcome this problem with the use of Boolean Operations, either the orientation of objects should be recalculated to obtain an undercut free orientation[38], or concave objects should be convexified before applying the Boolean operations. These techniques require prior knowledge of molding and considerable computational power. Furthermore, for a smooth packaging process and packaging mold creation, packaging designers also need to create an offset from the model as well as parting lines and a draft angle for packaging molds [11, 39]. Since those procedures often require experienced engineers to intervene, an automated method which can identify product packaging space is very desirable.

In this chapter, an efficient method for detecting packaging supporting surface is presented and discussed. This method can further provide the offset and draft features,



as seen in Figure 3-1(a), based on its simple data structure without undercut, calculation of parting information, and topology information. It can generate the supporting mold quickly and output as commonly used STL format or other format specified. A detailed discussion of the method is given in the next section. In section 3.3, three design examples are presented to demonstrate this procedure.

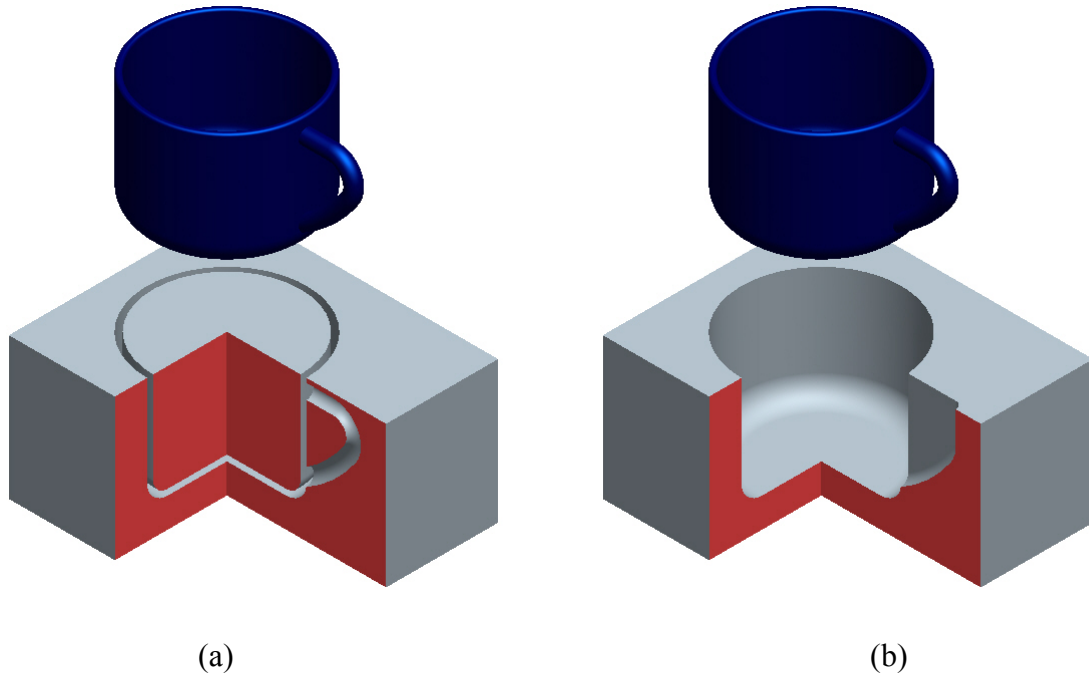


*Figure 3-2: Boolean Operation May Create Faulty Design for Concave Models  
(a) Faulty Design. (b) Valid Design.*

## 3.2 Packaging Supporting Space Identification

The method presented in this chapter is to generate packaging supporting space for a given product model with pre-specified product arrangement and a packaging bounding box. The resulting packaging supporting space can directly be translated into an undercut-free supporting mold for packaging foam and packaging assembly. It is worth noting that this method can identify the packaging space automatically without any prior

knowledge on parting algorithms to prevent interference between models and supporting molds.

There are three major steps in this method: (1) facet reduction, (2) height detection, and (3) surface generation. The facet reduction eliminates unnecessary calculation by reducing the number of model facets. The height detection creates an evenly distributed supports for products and removes undercut supports. Surface generation connects evenly distributed supports into a Non-uniform Rational B-Splines (NURBS) based surface model. It also includes offsets and draft angle for the molding operations. These steps are programmed using C# and are discussed in detail in this section.

### **3.2.1 Facet Reduction**

With pre-specified product arrangement and bounding box, a set of evenly spaced supporting lines is created from the bottom of the bounding box towards the products. Although there is no limitation on the spacing between supporting lines, it should be slightly smaller than the size of the smallest downward facing triangle such that all features of the product model can be captured. From our numerical experiments, using an eighty percent nominal length of the smallest feature as the spacing can always produce satisfactory results. Once the spacing is determined, a set of 2-D mesh grids can be generated on the bottom plane of the bounding box. These mesh grids are positioned as the starting points of the vertical supporting lines and the ending points are the intersections of supporting lines to the products as shown in Figure 3-3(a). Notice that the lines can go through the models at this moment because the height of each line is not determined here yet. The expected intersections between each supporting line and model will be calculated as shown in Figure 3-3(b). It is worth noting that the resultant

intersecting points should avoid the concave part of the model in order to create an undercut free supporting surface that will be based on the information obtained in this process.

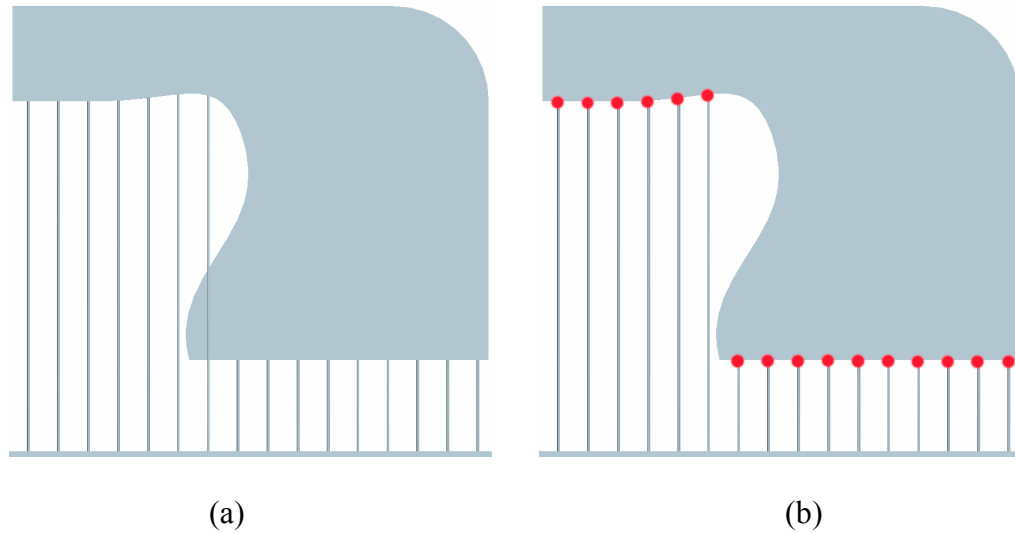


**Figure 3-3: Expected Height Detection Result Indicated in Red Dots.**

Since the products are often given or transferred in the form of surface representation, a commonly used data format, STL format, is implemented in this study. The STL file format simply describes the surface model of solid parts using continuous connected triangles that approximate the surface with little distortion, because a triangle is one of the basic graphic and geometry primitives. The distortion can be controlled and minimized by adjusting the angle and chord height control during the STL transformation.

Since the products are often given or transferred in the form of surface representation, a commonly used data format, STL format, is implemented in this study. The STL file format simply describes the surface model of solid parts using continuous connected triangles that approximate the surface with little distortion, where triangle is one of the basic graphic and geometry primitives. Each triangle in this file format is specified with

its three vertices, arranged in counterclockwise order, along with its surface normal calculated using the right hand rule from its vertices as shown in Figure 3-4. The surface normal vector is normalized to have unity length.

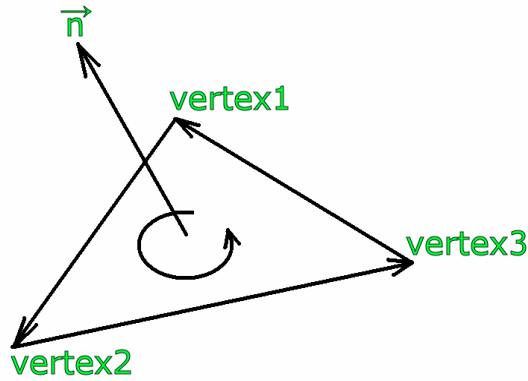


*Figure 3-4: Triangle Primitive of a 3D Model in the STL File Format.*

A typical ASCII data of a facet in a STL file has the following format:

<i>facet normal</i>	<i>u</i>	<i>v</i>	<i>w</i>
<i>outer loop</i>			
<i>vertex</i>	$x_1$	$y_1$	$z_1$
<i>vertex</i>	$x_2$	$y_2$	$z_2$
<i>vertex</i>	$x_3$	$y_3$	$z_3$
<i>endloop</i>			

where  $(u, v, w)$  represents the surface normal vector and  $(x_i, y_i, z_i)$  are the coordinates of the vertices. Although our algorithm assumes that products are pre-arranged and a well defined STL file or a set of STL models are given, the facets of STL models are not necessary to be organized with any particular order. Therefore, to calculate the intersection between all supporting lines to the products which require comparing all supporting lines with all facets is definitely not a trivial task.

In order to improve the efficiency of designing the supporting surface, the first step to reducing the computational effort is to eliminate unnecessary calculation during the

height detecting process by reducing the number of facets in the STL files for calculating. Considering the object as shown in Figure 3-5, it is obvious that all facets with green normal vectors need not be included in the intersection test.

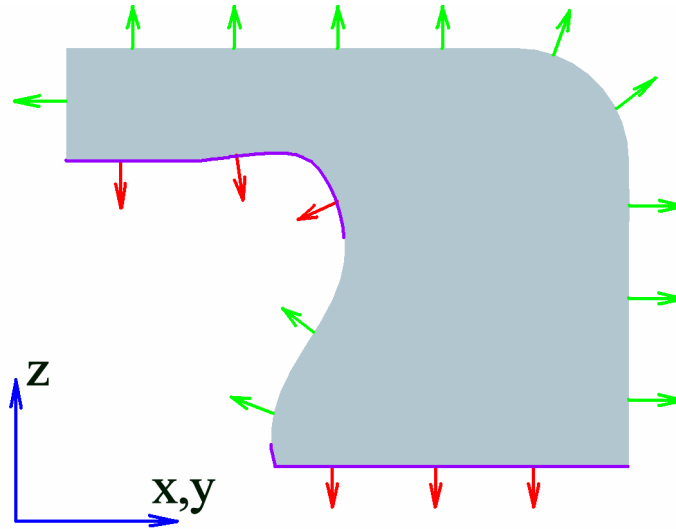


***Figure 3-5: All Facets With Green Normal Vectors Should not be Included in the Intersection Test.***

To remove all facets with a non-downward normal vector, we first need to transform all of the entities in the model to have the same coordinate system and then rotate the z axis to be the direction pointing upwards as the supporting lines. This is done by applying homogeneous transformation which is multiplying a series of 4 by 4 transformation matrices. Once these transformations are completed, all facets with a positive z component in the normal vectors should be dropped from the comparison pool. This selection process can reduce a great number of facets before the intersection calculation and only require very little amount of computational power.

After completing the aforementioned processes, the preparation for height detection procedure is accomplished. It is ready to apply the height detection algorithm on the grids and the facets.

### 3.2.2 Height Detection

For each supporting line, the height from the base to the product must be calculated. Although the number of facets has been greatly reduced as described in the previous section, there still has no obvious pattern to locate the corresponding facet above for each mesh grid. Hence, it is rather difficult and costly to evaluate the height directly from the mesh grid to find the facet right above. To solve this problem, we trace back the mesh grids from a given facet by projecting the facet onto the mesh grid plane. As an example shown in Figure 3-6, the red mesh grids enclosed by the projected triangle are the corresponding mesh grids that will be used to calculate the height / distance to the facet.

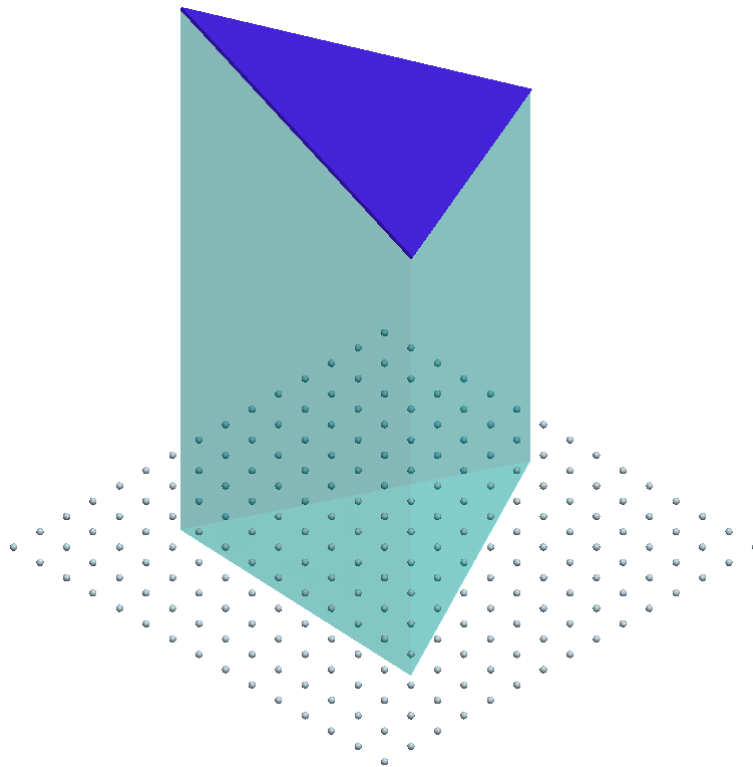


*Figure 3-6: Grids Enclosed by a Projected Facet along the Supporting Direction.*

Since it is also costly to determine whether grid is inside the projected triangle throughout all the grids, a pre-test using a bounding rectangle enclosed the projected triangle, as shown in Figure 3-7, is applied first to limit the grids to be checked. This pre-test is very easy because the mesh grids are pre-defined and spaced regularly. The maximum and minimum values of x and y coordinates of the three vertices of the projected triangle is obtained by simply compare the x and y values of the vertices. The bounding box of the projected triangle is then formed from the data. This procedure ensures that only the internal grids inside the bounding box will be checked to see if they are inside of the projected triangle.

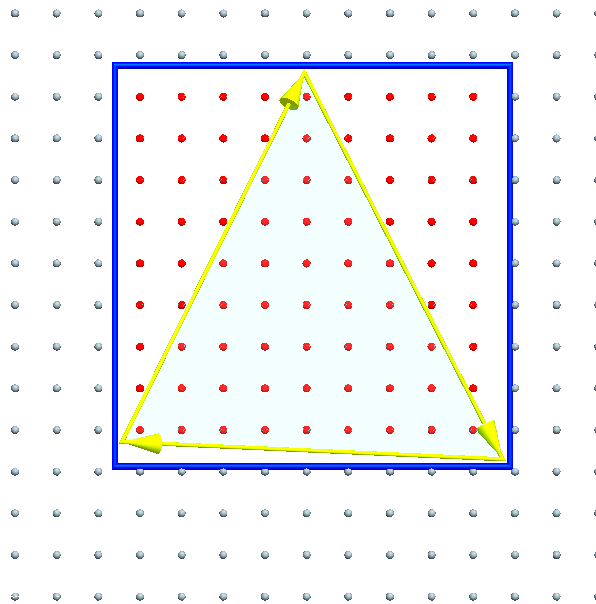


***Figure 3-7: Top View of the Projected Triangle of the Base of the Height Grid Mesh.***

At this point of progress, a very large amount of unnecessary grids have been dropped with very little cost of computation power. To verify whether the mesh grids are the corresponding ones for a given facet, the following procedure is used. If one looks from the top of the bounding rectangle, the projected triangle has its edge vectors run clockwise, as shown in Figure 3-7, because all the projected facets have their surface

normal pointing downwards. The inner grids will be always on the right side of every edge of the triangle. The easiest way to select the inner points is to compare the z value of the cross product between the edge vector and the vector formed by the end vertex and the targeting grid. When the z value of the outer product is less than or equal to zero, then the grid is inside the triangle as shown in Figure 3-8. This test is performed along each edge of the facet. If any of the tests fail to confirm the grid is inside the projected triangle, the point will be removed immediately.

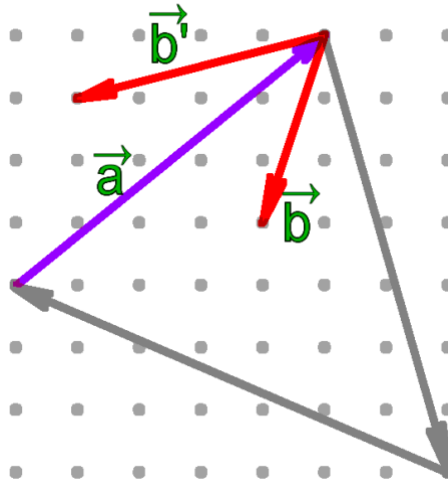


*Figure 3-8: Edge Vector and the Vector Formed by the End Vertex and Targeting Grid Are Used in the Inner Test.*

The computational cost for this process is also low because it only requires a few steps of multiplication and addition. A full outer product of the testing vectors needs not to be performed. Calculation of the z-component is sufficient and it is not more than a simple determinant.

After collecting all inner grids for each facet, it is rather straightforward to calculate the intersection point. The plane that embraces a given triangle with facet normal  $(u_k, v_k, w_k)$  can be defined as:

$$u_k x + v_k y + w_k z = u_k x_a + v_k y_a + w_k z_a \quad (3.1)$$



where  $(x_a, y_a, z_a)$  is one of the vertices coordinates of the facet. The z coordinate at the product end of the supporting line with respect to a mesh grid  $(x_i, y_j)$  can be calculated easily as:

$$z_{i,j} = z_a + \frac{u_k(x_a - x_i) + v_k(y_a - y_j)}{w_k} \quad (3.2)$$

In some cases, when a supporting line is going through a concave part of the model, it may intersect with more than one facet. In this case, the shortest height will be assigned to be the actual height on that grid to avoid penetration, as shown in Figure 3-9.

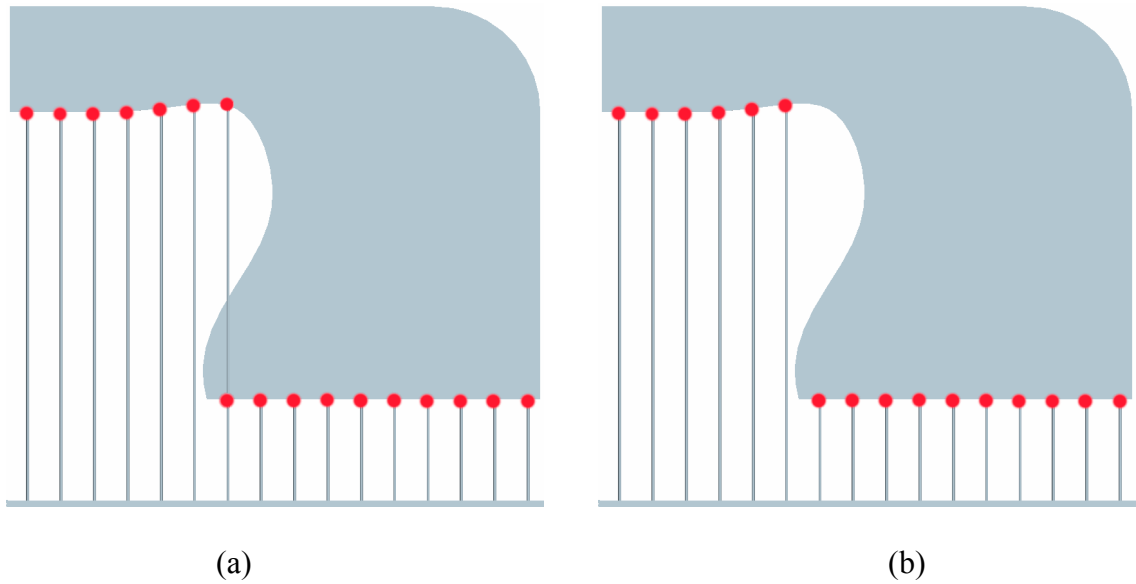


**Figure 3-9: Height Adjustment when Multi Crossing Cases Occurs to Avoid Undercut.**

After finishing the process described in this section, the height information is obtained between all the mesh grids to the model(s). It can be used to form a smooth surface as the supporting surface of the packaging tray. The procedures and algorithms of generating a smooth surface for the packaging tray will be presented in the next section.

### 3.2.3 Surface Generation

Although the heights of all supporting lines from the mesh grids are obtained after the height detection, the packaging supporting surface still cannot be formed by simply connecting these points because there are some portions of the models may have interference as shown in the red lines of Figure 3-10(a). It can be noticed that the lower middle part of the model has little interference with the direct connected surface patch.

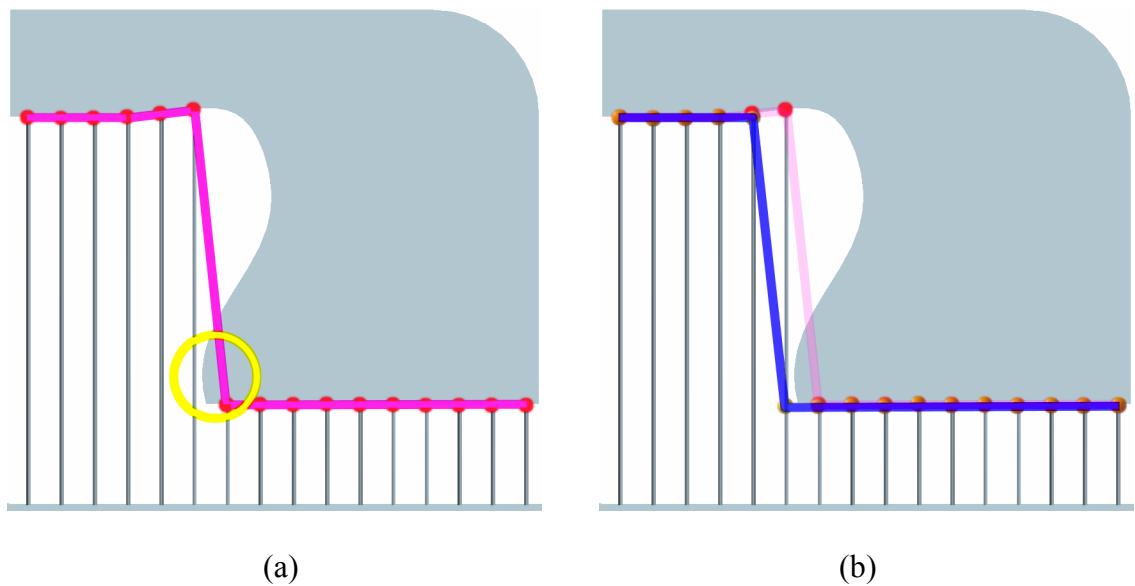


**Figure 3-10: (a) Direct Connecting of Mesh Grids Results in Minor Undercut. (b) Height Relaxation Can Avoid This Effect.**

In order to overcome this problem, heights of supporting lines at the location where surface normal changes from down facing to up facing may be relaxed. In this study, an efficient and effective height relaxation method is implemented. For a given supporting line, we compare all possible eight neighboring supporting lines for their heights and the lowest value among all neighboring heights is assigned to be the new height. This method applies to every supporting line to adjust its height to a new one if needed to avoid interferences. After the height relaxation method, all new heights can

be connected to form a supporting surface as shown in the blue lines of Figure 3-10(b). The height relaxation method should be performed again for the next smoothing filtering. To further smooth the supporting surface, a linear smoothing filter is applied. The size of the smoothing filter mask controls the amount of filtering. A larger convolution mask results in a greater degree of filtering, therefore, a loss of details. In this study, a single peak 3 x 3 linear smoothing filter is used:

$$\begin{bmatrix} w_1 & w_2 & w_3 \\ w_4 & w_5 & w_6 \\ w_7 & w_8 & w_9 \end{bmatrix} = \frac{1}{16} \begin{bmatrix} 1 & 2 & 1 \\ 2 & 4 & 2 \\ 1 & 2 & 1 \end{bmatrix} \quad (3.3)$$

Normally, linear smoothing filters remove high-frequency features and the sharp detail is lost. This effect is actually very advantageous in defining the supporting surface with a moderate offset and draft angle. Furthermore, this filtering process can be repeated till the desired tolerances for offset and draft angle are achieved. An example of the final supporting surface plotted in the green lines is shown in Figure 3-11.

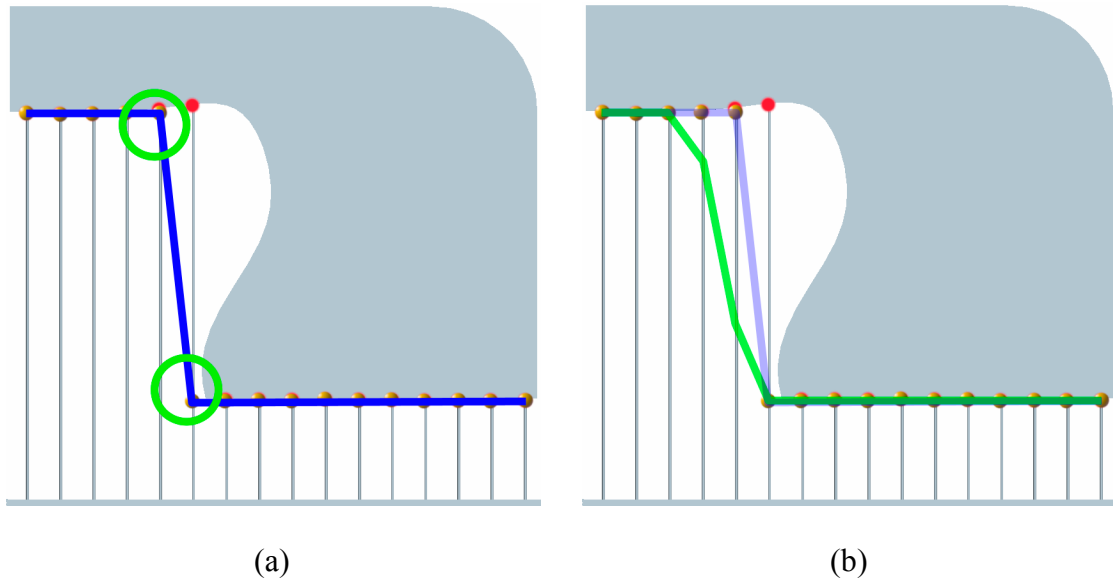


**Figure 3-11: (a) Sharp Edges Exist on the Connected Surface. (b) Sharp Edges Reduced After Applying Smoothing Filter.**

Supporting surface created by simply connected lines will have small sharp corners or cliff shapes even after smoothing filtering. These sharp corners or cliff shapes are not desirable in fabricating the supporting molds. Therefore, a NURBS surface defined as follows is used to remove these undesirable features[40, 41]

$$S(u, v) = \frac{\sum_{i=0}^n \sum_{j=0}^m B_{i,p}(u) B_{j,q}(v) P_{i,j} w_{i,j}}{\sum_{i=0}^n \sum_{j=0}^m B_{i,p}(u) B_{j,q}(v) w_{i,j}} \quad (3.4)$$

After NURBS converts the line-connected surface to a continuous surface representation, this surface is used to generate the supporting molds. The smoothed surface is shown in Figure 3-12. In this study, the STL format is used to export this surface to an RP machine for fabrication. In the next section, three examples are presented to demonstrate the results from our proposed method.

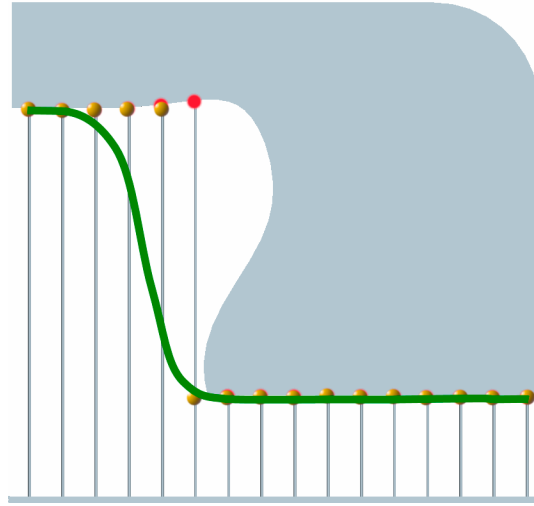


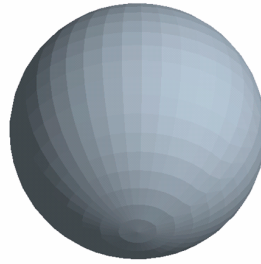
*Figure 3-12: A Smoothed Connected NURBS Surface Is Shown as the Green Line.*

### 3.3 Examples

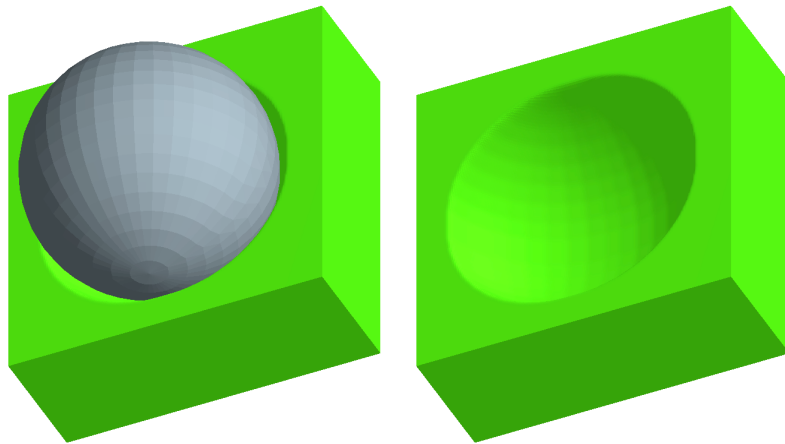
This method is implemented using C#.NET on a Pentium 4 2.66GHz personal computer with 1.5GB RAM. Three models are used to demonstrate this proposed method. The first example is a simple convex object. The second example is a more complex model with multiple components. The third example is one with a very large number of facets for the efficiency test. They are presented in this section.

#### 3.3.1 Example 1: A Ball Model

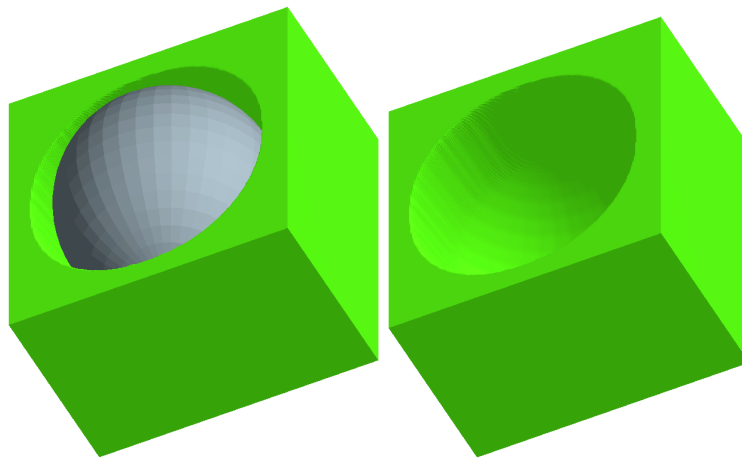
A simple ball model is presented in the first example because it is a strictly convex model. The ball contains 1596 facets and the bottom of the supporting space is divided into 200 by 200 mesh grids as shown in Figure 3-13(a). First, the height of the bounding box is chosen as 45% of the diameter of the ball, which is slightly below the center of ball. A concave supporting space is generated in 0.075 second in a personal computer as shown in Figure 3-13(b). When the height of the bounding box elevates to 70% of the diameter of the ball, a simple negative model using Boolean operation cannot be used as the supporting space. However, our method can still produce a useable supporting space automatically by creating a cylindrical cavity after the supporting space passes the half ball as shown in Figure 3-13(c). The entire operation is completed within 0.081 seconds.



(a)



(b)



(c)

**Figure 3-13: (a) A ball model with 1596 facets, (b) Supporting space for a bounding box with height of 45% of the diameter of the ball, and (c) Supporting space for a bounding box with height of 70% of the diameter of the ball.**

### 3.3.2 Example 2: A Suspension Model of a Remote Controlled Car

In the second example, a remote control car suspension model is used. This model consists of fifty five (55) individual components: wheels, motor, transmission gears, differential gears, frames, etc., totaling 140,640 facets. Those models are shown in Figure 3-14. A mesh grid (300 x 524) are created in the bottom plane of supporting space. The height of the bounding box is chosen as the 75% of the height of the car. Although parting lines of this example are not as uniform as the previous one, the height detection can still generate all correct parting lines automatically. The final supporting space is generated in 0.83 seconds. The results are shown in Figure 3-15.

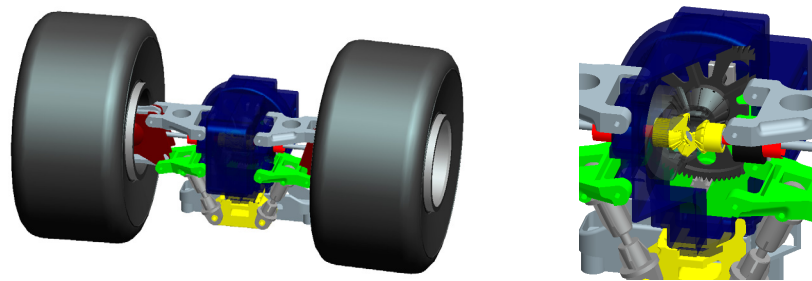


*Figure 3-14: (Left) A Suspension Model. (Right) A Closer Cut-away View of the Internal Components*

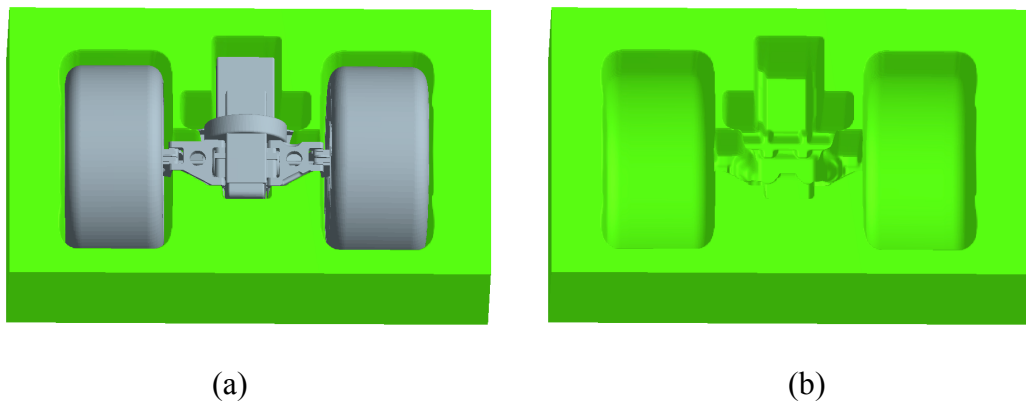


*Figure 3-15: (A) Suspension Model and Supporting Space with 70% Height, (b) Supporting Surface.*

### 3.3.3 Example 3: A Dragon Model

Finally, a dragon model with 871,414 facets is tested. This model can be retrieved from the Stanford 3D Scanning Repository (<http://graphics.stanford.edu/data/3Dscanrep>). It is transformed into an STL file format from its native PLY (polygon) format. The supporting space is divided into 300 by 425 mesh grids. The height of bounding box is chosen as 70% of the height of the dragon. The final supporting space is generated in 1.80 seconds and the result is shown in Figure 3-16. This shows that the height detection procedure developed in this method is very efficient regardless the complexity of model surface.

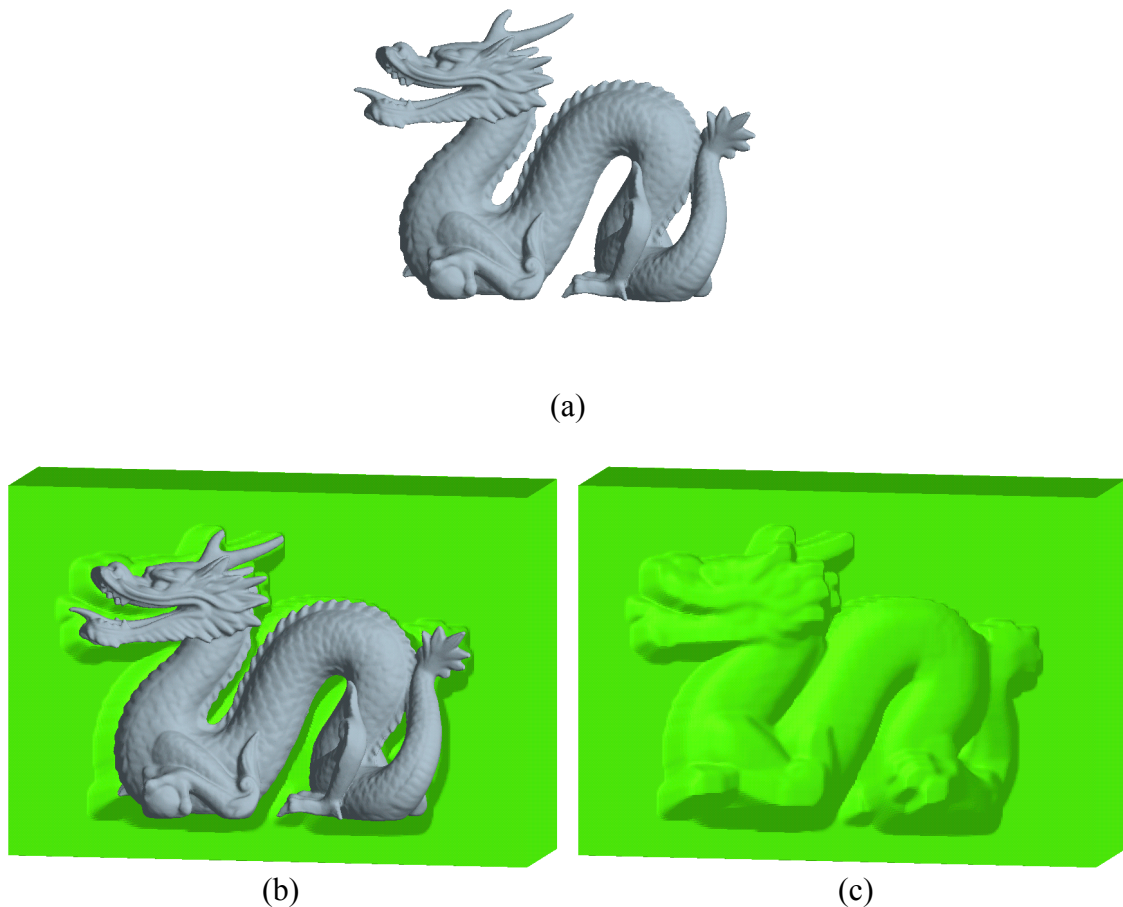


*Figure 3-16: A Dragon Model with Flat Base Facing Down.*



### 3.4 Efficiency Tests

The algorithms described in this chapter are designed to have outstanding efficiency. The main methods of achieving this goal are to design a light data structure and eliminate unnecessary calculations throughout the whole process. To demonstrate the efficiency of these algorithms, a simple ball model similar to the one in the example 1 and the dragon model in the example 3 are used here. The ball model is generated and saved to have a different number of facets and the supporting space is divided into different amount of grids to compare the time required to generate the supporting surface. The results are shown in the following tables and figures, and are discussed in this section. The first test is to compare the time spent on ball models with different number of facets when the base grids are set as constant.

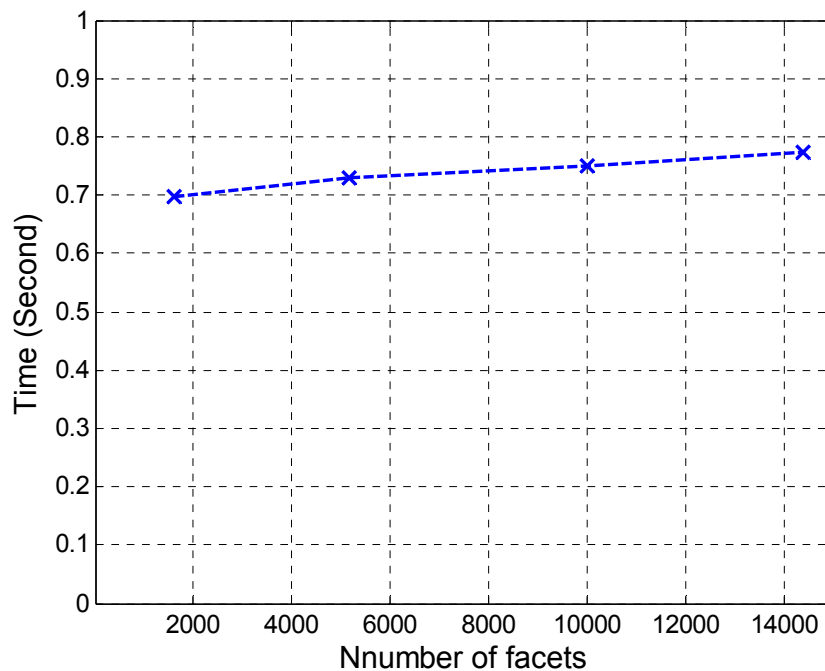


*Figure 3-17: Efficient Test Results on Different Number of Facets of the Same Ball Model.*

As shown in Figure 3-17, the ball model is exported into several versions with varied amount of facets. Fifty percent of the height is designed to be covered. Half of the facets are down facing and are used to generate the supporting surface. The result shows that despite the number of facets varies from approximately three to nine times compared to the smallest one, the consumed time for obtaining the supporting surfaces increased only about 10 percent. This concludes that the number of facets plays a minor role to the same model. This conclusion can be expected since the use of the number of the facets is only to find the grids each triangle included and the algorithm for finding those grids involves only a few steps of multiplication and addition.

***Table 1: Efficiency Test Result of a Simpler Ball Model with Different Grid Configurations***

Number of facets	Supporting grids	Consumed time
1,596	100 x 100	0.035143
1,596	200 x 200	0.154154
1,596	300 x 300	0.376347
1,596	400 x 400	0.698537

In Table 1, a simpler ball model is used to create the supporting surface with different grid configurations. The result shows that the time spent on finding the resultant supporting surface is somewhat more than expected as the change in complexity of the number of the grids. The complexity calculated from the table may not be linear here. This effect is also expected on simple models because each model needs to go through some data preparation, such as memory allocation and data structure conversion, before it enters to the calculation algorithms. The data preparation time but does not play a major role on simple models. A more complex ball model is used to prove the point aforementioned. This ball model has 14,396 facets which are nine times of the simpler model. The resultant time table is shown in Table 2. It can be seen from Figure 3-18

that the result is actual linear but does not go across origin point because of the initialization time is always required for models.

**Table 2: Efficiency Test Result of a Complex Ball Model with Different Grid Configurations.**

Number of facets	Supporting grids	Consumed time
14396	100x100	0.063718
14396	200x200	0.203873
14396	300x300	0.436797
14396	400x400	0.774211

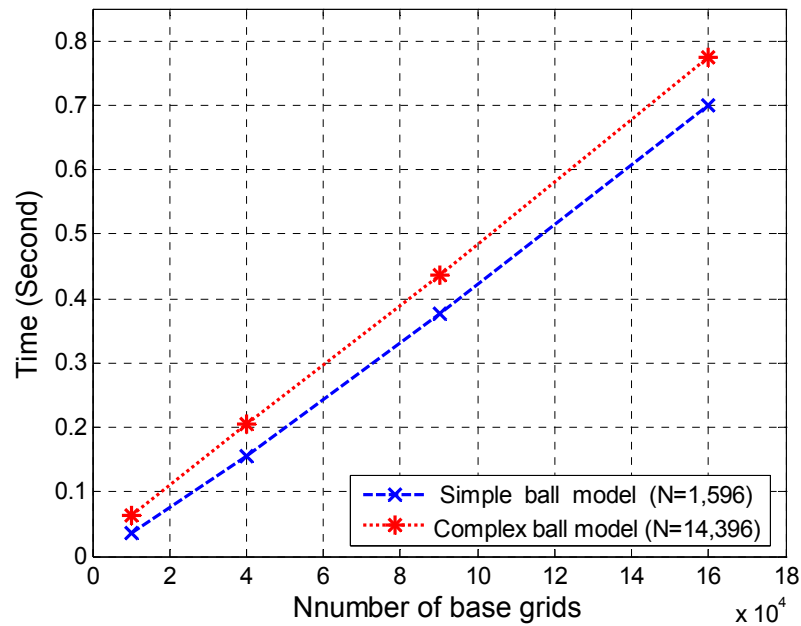


**Figure 3-18: Efficient Test Result on Ball Models with Different Number of Supporting Base Grids.**

The test result on another more complex model, the dragon model with 871,414 facets, indicates the efficiency is somewhat better than linear. The result can be found in Table 3 and Figure 3-19. In Figure 3-19, test results of the simple ball model, complex ball model, and the dragon model are illustrated. It is worth noticing that although the dragon model has approximately 550 times of facets, the time difference is less than 50 times. This again confirms that the number of facets of the model has a minor effect to

the algorithm described here which means this algorithm is capable to handle practical commercial applications.

**Table 3: Efficiency Test Result of a More Complex Dragon Model with Different Grid Configurations.**

Number of facets	Supporting grids	Consumed time
871414	100x142	1.755489
871414	200x284	1.991360
871414	300x425	2.511812
871414	400x567	3.156306
871414	500x708	3.946600
871414	600x850	4.793708
871414	700x992	5.671874
871414	800x1133	6.520663
871414	900x1275	7.670200

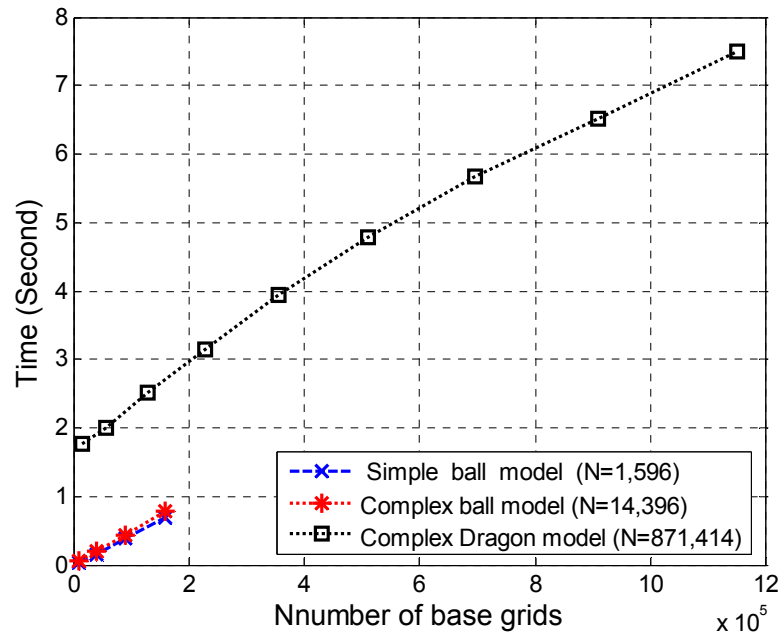


**Figure 3-19: Efficiency Test Results on Different Models.**

### 3.5 Conclusion and Remarks

An efficient method for generating packaging supporting surface has been presented in this chapter. This method can identify the packaging space automatically without any

prior knowledge on parting algorithms to prevent interference between models and supporting molds. The efficiency of the algorithm developed in this study is a less-than-linear complexity algorithm. Its speed depends on the number of down-facing facets of the model and mainly the size of mesh grids. Consequently, the time needed to create a supporting surface for a complex model can be expected in a reasonable short time frame. The only limitation of this method is that a well connected surface model is required. There are many algorithms to patch those models with missing facets available or with faulty assigned facet normal [42].

## Chapter 4.

### Design of Thin-walled Packaging Structures

#### 4.1 Introduction

Thin-walled packaging structures in the industrial packaging field usually refer to thin polyethylene packaging and molded pulp. Both polyethylene and molded pulp are used to hold products and all its accessories within a pre-defined arrangement. Polyethylene is used in the scenario that transparency is demanded for a better representation of the products. It is usually not applied to products which are heavy and sensitivity that require superior support and protection. Molded pulp is more commonly used in the industry as a heavy duty packaging type [43-45]. An example of an application of molded pulp on consumer electronics is shown in Figure 4-1



*Figure 4-1: An Example of Molded Pulp for a Printer. (<http://www.enviropak.com>)*

Pulp molding is not a new concept. It actually originated in China several thousand years ago when bamboo and other plant fibers soaked in limewater were pounded into

pulp to be used in making paper, masks, kites and models. The main processes of paper making remained unchanged until the 19th century when chemists and engineers found ways of producing larger quantities of pulp at a consistent quality and a reasonable cost [43]. The mold for papermaking has a flat shape so that a paper can be formed when it extracts water from pulp mixture. Complex shapes can be formed from pulp mixture by applying mold that has desired shape such as masks. Thus this concept, conducted in the packaging industry, is called molded pulp or pulp mold. The use of molded pulp as a dunnage or commodity material in packaging goes back to World War I. But only in the past few years have packaged goods manufacturers begun to design molded pulp to meet specific applications such as Industrial Packaging [44]. The molded pulp packaging and container materials used today are manufactured using 100% pre and post consumer newspaper, kraft paper and other selected waste papers as well as agriculture waste. They are fed into the pulping machine and mixed with water. Inside, paper is chopped into small pieces. At this stage, the pulp looks like a thick gray porridge. Then, natural waxes and binders are added to ensure the final integrity of the finished products. This means the product is able to withstand fluid leakage for weeks. The mixture undergoes a final screening and additional mixture of water to bring it to the correct consistency for the molding process.

After getting the pulp mixture ready, a set of well-utilized molds will be soaked into pulp and vacuum the water away. The pulp near the mold will become dense and finally attached on the molds. By removing the mold module out of the pulp tank, a half dried molded pulp is obtained by exhaling air out of mold. The next step of making molded pulp is the drying process and post manufacturing such as waxing, cutting, etc.

depending on the final purpose of the product. Figure 4-2 shows the basic process of making molded pulp. A set of well-designed molds is the most important component in the process. In the molded pulp industry, there are some computer-aided design software packages used in designing molds. However, they are usually general CAD software and not specialized for pulp mold design. There are many parameters that will affect the final result of molded pulp. Thus, to operate this kind of general purpose software requires well-trained experienced engineers. Since molded pulp is expected to be a main packaging material in the next few decades, well-developed mold design software is needed at this point of time so that it can be used to design thin wall structure automatically. The software should be able to take CAD models and automatically generate a mold which can form an optimized supporting thin wall structure for packaging.

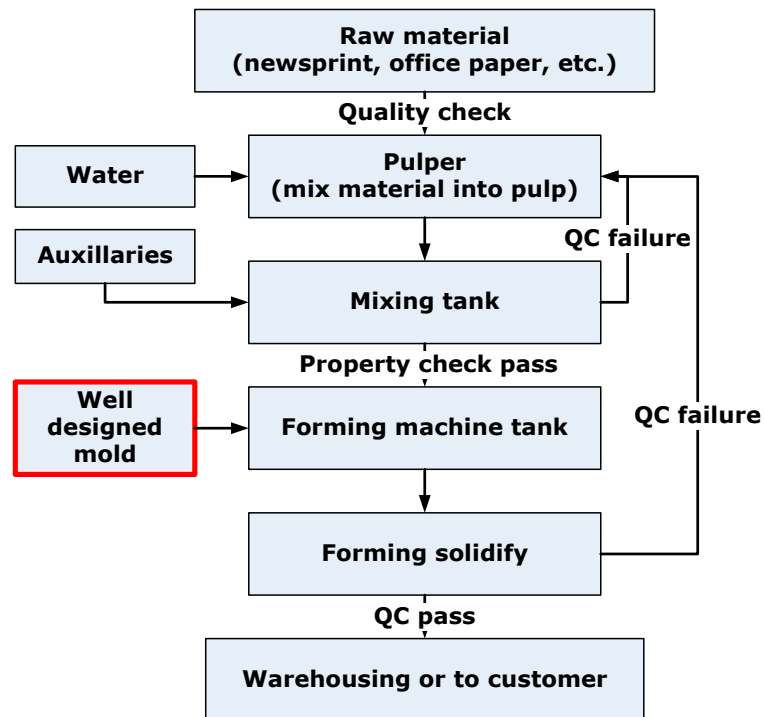


*Figure 4-2: Process of Making Molded Pulp.*



## 4.2 Benefits of Using Molded Pulp

All of the materials used for making pulp are 100% recycled or all natural. The recycled material includes newsprint, cardboard, and office papers. The aforementioned material is basically collected from household and office recycling. It can be used to produce paper-based product directly without tedious procedures. Agriculture waste such as straw can replace recycled paper to skip the purifying processes. Furthermore, paper recycling is in the most efficient reusable category. For instance, the recycling rate of paper is much more than that of plastics. Reducing pollution is not the only purpose of using molded pulp. There are still lots of benefits of using it. Such as the following: [43, 45, 46]

### 1. *Environmental friendly:*

- **Acquirability:** As aforementioned, material of making molded pulp is mainly all from recycling paper. Most communities in the US have paper recycling programs. Different types of paper even being recycled separately. Thus, it is very easy to obtain the raw material.
- **Reusability:** Molded pulp products are essentially 100% recyclable material.
- **Decomposability:** Molded pulp products can be decomposed in 40 days when disposed in a landfill. Also, there is no toxic substance emitted during decomposition or burning.
- **Compatibility:** Many countries have their environmental protection policies for domestic and international standards. There are many restrictions against pollutant materials as well. Molded pulp is prospected to conform to the international environmental protection standards.

## 2. *Product competitiveness:*

- Shock absorption: Molded pulp can offer superior support to the product enclosed in it. By designing the supporting pattern and thickness, different levels of shock absorption and suspension can be provided.
- Warehousing: Molded pulp is practically a thin wall type product. Due to the design of mold and draft angle consideration, it can be stacked up and save up to 70% warehousing space. Figure 4-3 illustrates the space saving feature of molded pulp.



*Figure 4-3: A Picture Showing Space Saving Feature of Molded Pulp.*  
 (<http://www.enviropak.com>)

- Downsizing package: The one dominance of pulp mold characters is thin wall structures. That can make for smaller volume after packing and also provide equivalent strength. For this reason it is easily filling up in high transportation efficiency.

## 3. *Wider application:*

- Molded pulp can be used for various applications such as egg trays, fruit trays, food containers, industrial packaging, etc. Those products packaged with plastic material will be soon replaced with environmental friendly materials. Molded pulp is a competitive candidate.

### **4.3 Challenges to Molded Pulp**

The molded pulp industry currently is mainly focusing on manufacturing and tries to improve their productivity and manufacturing capacities as well as discover new materials. Accurate and fast machines with larger tank capacity are being used for productivity improvement. The productivity power is quite enough for current market orders. Furthermore, some new materials have been discovered for making food containers or medical equipments because they require higher hygiene levels. Those materials include sugar cane bagasse, phragmites communis, straw pulp, bamboo pulp, and wood pulp, which are all natural fibers. They need fewer processes to purify. As for industrial packaging, recycled paper is the main raw material. It is much cheaper to get and handle than plain fibers because paper recycling program is also one of the most efficient recycling programs.

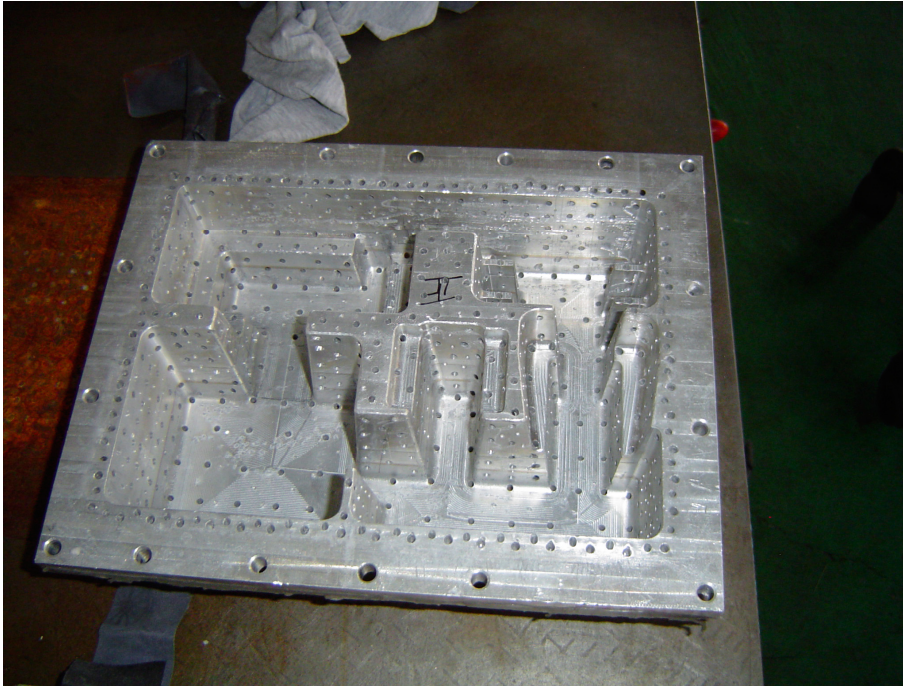
In industrial packaging, according to various requirements and the characteristics of objects to be packaged, there are some different covering types to fulfill those needs. These covering types can be divided into single and multi pieces. For single piece coverings, all products and their accessories are arranged in a single piece supported molded pulp. For multi piece coverings, some types can be found such as upper-lower, two sides, corners, etc. the possible covering types are trays, end-caps, cushions, clamshells, corner guards, pads, custom pallets, blocking, bracing and molded pulp specialties.

The molds design of the molded pulp industry is mainly operated by senior experienced engineers on general purpose CAD workstations. It requires practical experience to precisely create ribs and supporting patterns for a better suspension as well as some mold

related parameters. Sometimes, two sets of molds will be needed in forming a better surfacing molded pulp [44]. One is called forming mold which is used to form the shape of molded pulp and the other is called Thermo Forming Mold which is used to heat up the mold cast for forcing it to dry and compress it to get better strength. Also these molds have different gap allowance. These mold CAD models are usually sent to CNC tooling machines for manufacturing. After machine tooling, the molds need some finishing/post-processing such as adding mesh for forming molds and polishing for Thermo-Forming mold. The mesh added on forming mold is to allow water being extracted out from tank and form a semi-solid shell on mold. Figure 4-4 shows the mesh added on the forming molds. Notice that there are a lot of drain holes on the forming mold in order to extract water.

Again, there is no complete software package yet that can automatically formulate a mold design to enclose the products/CAD models, which will be packaged. Thus, this proposal suggests developing comprehensive software and systematic analysis methods to fulfill this need for industry.

This chapter discusses the methods to automatically generate mold design space for molded pulp and apply topology optimization methods discussed in chapter 2 to formulate suggested locations where reinforcement should be added. The mold design and optimization methods in this chapter will take the supporting surface generated in the previous chapter and form a thinned design space and apply the topology optimization method onto the design space to indicate the reinforcement locations on the thin space.



(a)



(b)

*Figure 4-4: The (a) Forming Mold and the (b) Mesh that Will Be Added onto it.*

## 4.4 Obtaining Design Space

Topology optimization processes are used to evolve from the current design to better designs which are specified by design variables. In topology optimization and finite element analysis procedures, all of the design variables are the volume density of each element of finite element mesh. Hence, a thin-walled design space for both finite element analysis and optimization procedures is required.

The design space generated in this study is a finite element mesh with a regular brick shape. The mesh is based on the height information detected using the methods described in the previous chapter which was designed to generate molded foam. The mesh is composed of hexahedron (CHEXA bricks) as defined in Nastran BULK data format, as illustrated in Figure 4-5. The definition of a CHEXA element is that a solid element made up of eight GRID points or can be defined in terms of three vectors R, S, and T, which join the centroids of opposite faces [47]. A continuous connected layer of CHEXA mesh is required to prevent pivot effect which will behave like hinges. It is defined to be continuous if there are more than three faces (include three) to share the face with other elements except for the elements on the four corners of the thin layer of the mesh as shown in Figure 4-6.

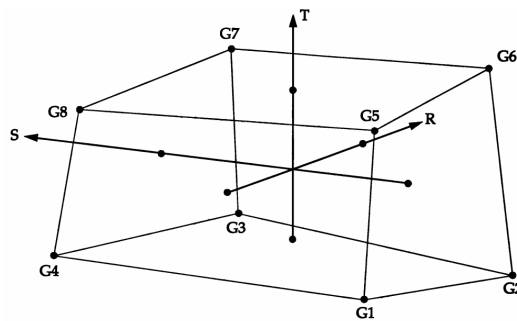


*Figure 4-5: An Illustration of HEX8 / CHEXA Element Defined in Nastran Bulk Format.*

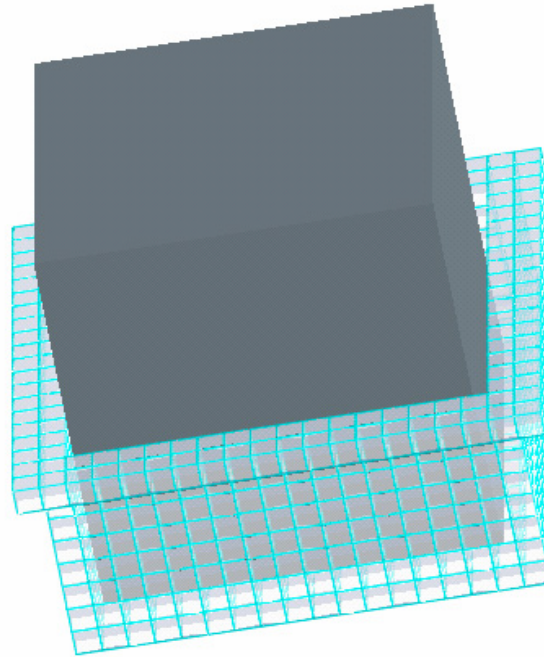


***Figure 4-6: An Example of Continuous Mesh for a Simple Box Model.***

To form a continuously connected mesh without the pivot effect, a set of four neighboring height grids is used. For grids with the same height, simply connected mesh can be formed. However, for grids with different heights, the lowest height value of the set of grids is chosen as the base height and an array of connecting hexahedron is generated from the base to the top, as shown in Figure 4-7.

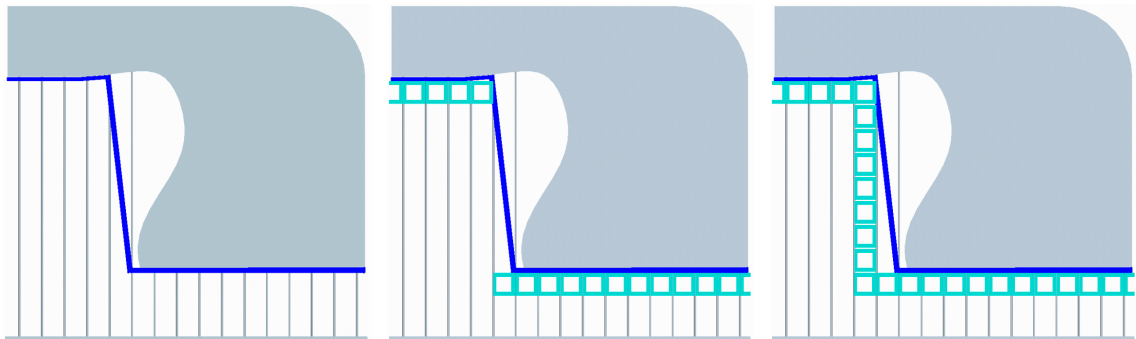


***Figure 4-7: An Example of Forming a Thin and Continuous Connected FEA Mesh Layer.***



All of the finite elements defined in this method are hexahedrons which are defined as CHEXA in the MSC Nastran data card. One might argue that other types of elements can be filled into the gap between the blue line and the mesh layer to make the mesh more close to the model. However, this scheme will cause more difficulties in meshing the design space and might have elements with a larger aspect ratio therefore cause some inaccuracy during the finite element analysis process. As an approximation to gain the ideas of locations to place reinforcement, a mesh composed of hexahedron is believed to be efficient and accurate in this application.

The completion of forming a finite element mesh is followed by applying finite element analysis onto this mesh to obtain stress and strain tensors which will be used in sensitivity analysis for topology optimization. In finite element analysis, a set of constraints and loads need to be defined under the designers' intention or knowledge. These processes will be discussed in the next section.

## **4.5 Applying Topology Optimization**

Once the thin-walled design space is generated, the designers can assign proper boundary conditions including supports and loadings to simulate various packaging conditions. Because thin-walled structures have very low stiffness against off-plane loading and vibration, they are normally reinforced by proper placement of stiffeners. There are two research directions related to the optimal stiffener design: the composite structure optimization problem and the reinforcement problem. The former models the thin-walled structures using orthotropic material and calculate the optimal thickness and orientation of orthotropic materials [48-52], and the latter utilizes the topology optimization to identify the optimal locations and orientation under various static and



vibration applications [53-59]. Since the main purpose of this paper is to demonstrate an automated design methodology of thin-walled packaging structure using topology optimization, only the mean compliance formulation is used to demonstrate the applicability of the method. In this paper, a microstructure-based design domain method is employed to formulate this problem due to its simplicity [30] and the optimization problem is solved iteratively by Generalized Convex Approximation [60]. This method has been implemented using C#.NET on a Pentium IV 2.66GHz personal computer with 1.5GB RAM. In the next section, examples of automated packaging design using this method are presented and discussed.

## **4.6 Design Examples**

Two examples are presented in this section. These two examples are thin-walled packaging structures: example 1 is a simple box and example 2 is a toy car model with multiple components. Designs of optimal reinforcement of both models using topology optimization under mean compliance formulation are presented. In order to simulate the stiffener locations on a thin-wall design space, a lower limit of density to elements is specified to represent the locations without stiffeners.

### **4.6.1 Example 1: A Simple Box Model**

A simple square box model is presented in the first example for a thin-walled packaging structure design because it is a simple convex model. First, the box is placed in a bounding space that is 30 percent larger along all its edges. A bounding plane is set at the height equals 50 percent of the total height as shown in Figure 4-8(a). Then the height detection grid is defined to have 30 x 30 points and the heights are accordingly

obtained as shown in Figure 4-8 (b). Followed by the design space generation, a thinwalled design space is obtained as shown in Figure 4-8(c).

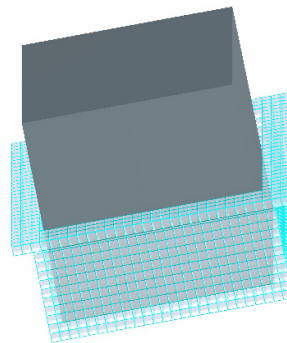
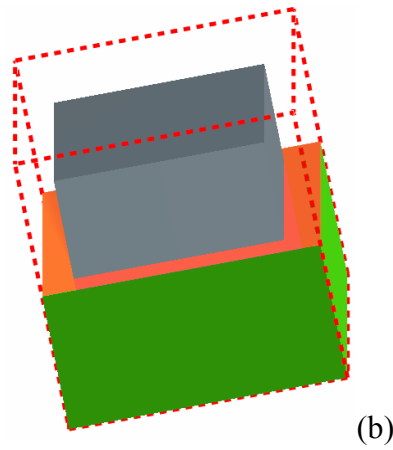
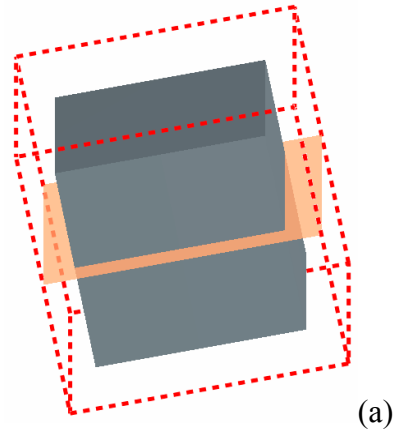


**Figure 4-8: A Box Example of Topology Design Space Detection.**

The loadings and constraints are assigned by designer according to its applications. As an example to demonstrate this method, a simply supported four corners are modeled with a concentrated load at the center of the bottom plane as shown in Figure 4-9(a). The allowable volume constraint is 15 percent of total volume onto the base thin layer with uniform density as 0.1. A set of symmetric constraints for x- and y- directions is specified. The optimization process is converged at 35 iterations and the final optimal reinforcement is shown in Figure 4-9(c) and Figure 4-9 (d).

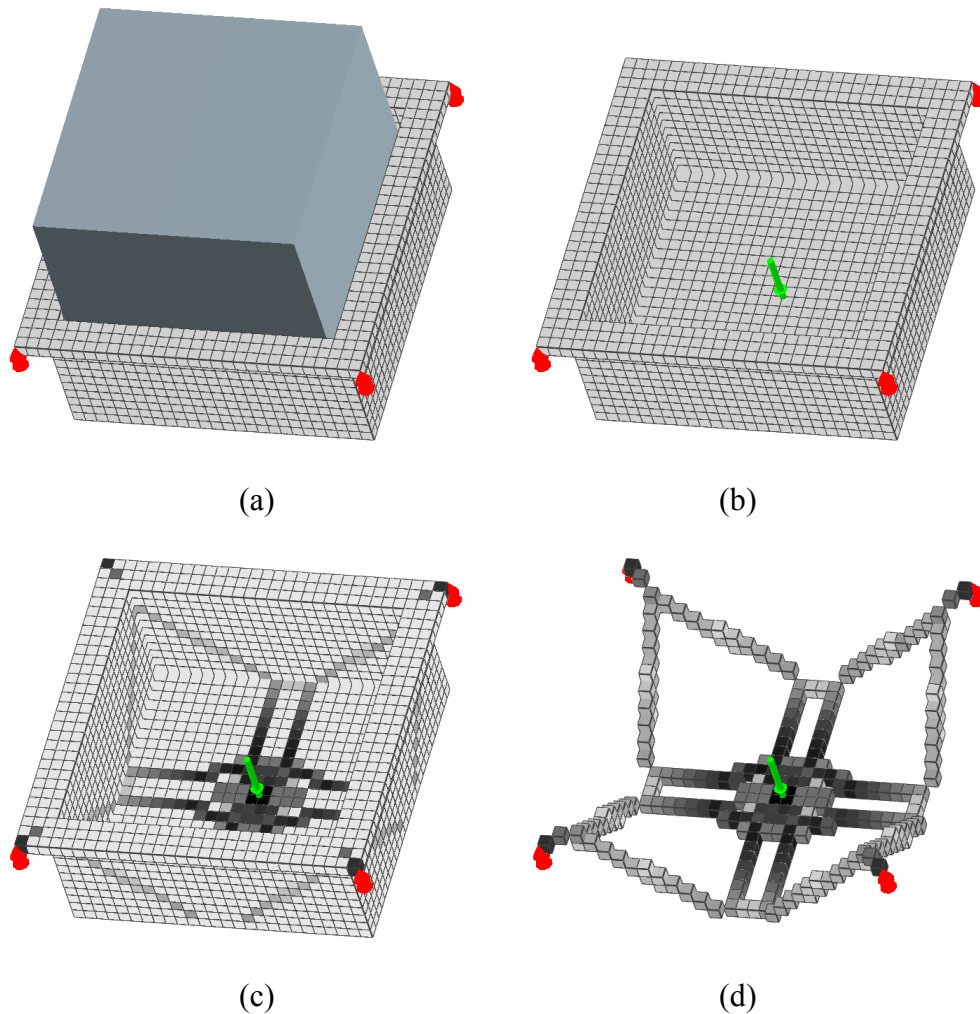
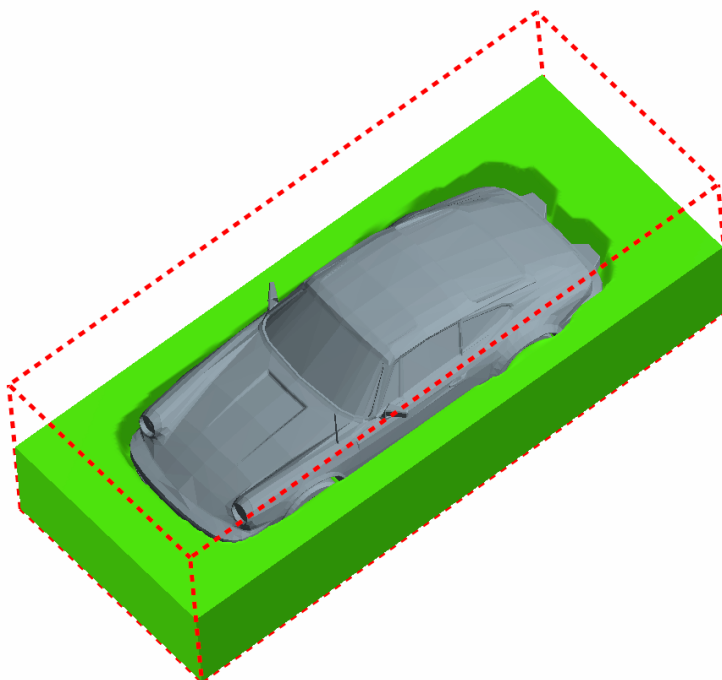


**Figure 4-9: Topology Optimization Result for the Box Model. (a )& (b) Design Space. (c) Result of Locations to Add Reinforcements. (d) Result with Material Densities Less Than 0.1 Removed.**

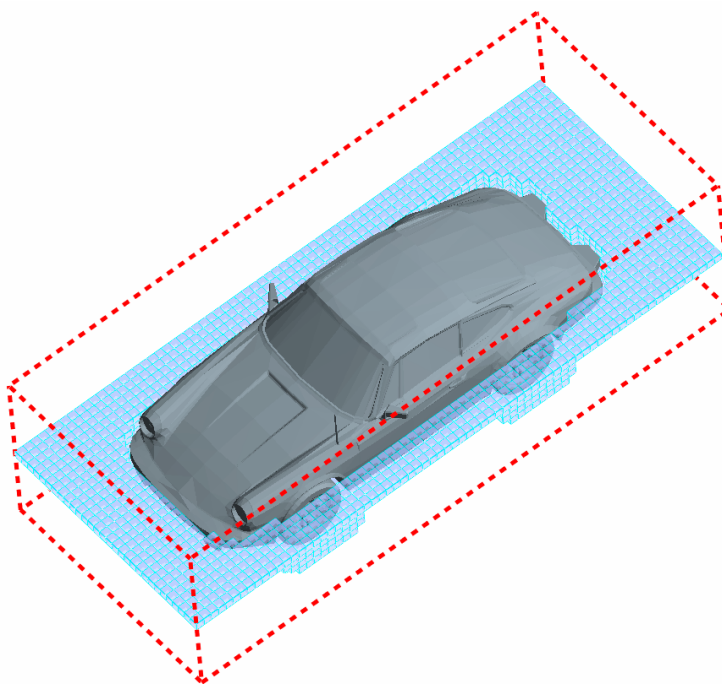
### 4.6.2 Example 2: A Toy Car Model

The other example is a more complicated toy car model because it consists of many small components such as a car body, four wheels, and two fog lights. Similar to the procedures described in the first example, the height is also set to 50 percent of the total height of the bounding box and the mesh grids are defined to be 30 x 72. A foam packaging space can be obtained after height detection as shown in Figure 4-10. Note that the foam packaging space is an under-cut free structure and was generated in less than 0.05 second.

The design space generation procedure is applied to the height mesh and forms a thin-walled design space. Four corners of the design space are fixed and the loadings are evenly distributed on four wheels. A mean compliance formulation is used and the volume constraint is set as 15% of the total volume onto a uniform thin layer design space with base density as 0.1. A horizontal symmetric constraint is applied. Topology optimization process converged in 63 iterations. The results of the optimal reinforcement for the thin-walled packaging structure with and without the toy car are shown in Figure 4-11. Another set of optimization with different boundary conditions is shown in Figure 4-12. From this two set of results, it can be noticed that the boundary conditions varies the optimal topology greatly. Thus, the design engineer should provide those boundary conditions with caution and need to ensure the accuracy of those assumptions on the conditions.



(a)



(b)

*Figure 4-10: Height Detection and Design Space Generation for a Car Model.*

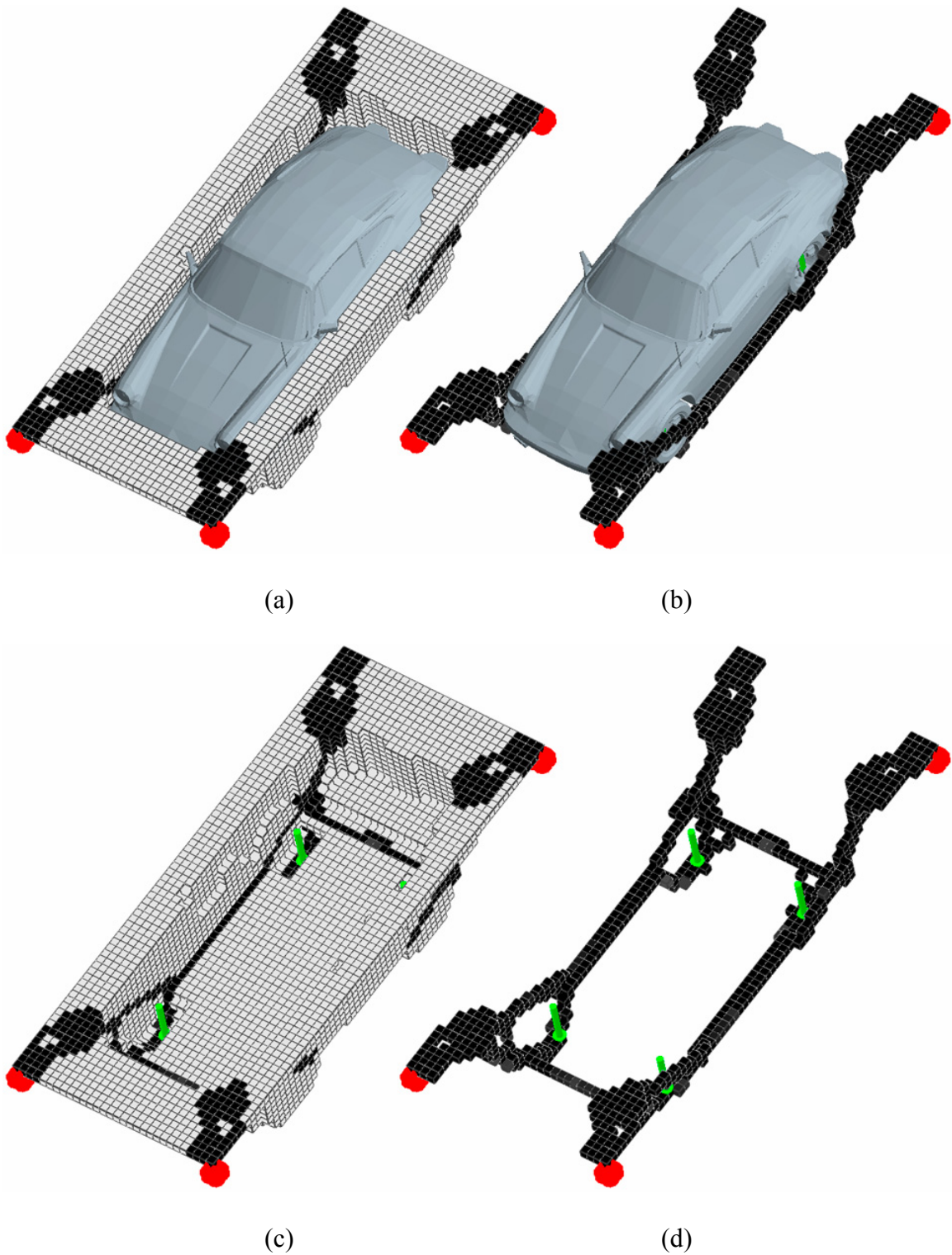


**Figure 4-11: Result of Topology Optimization for a Car Model: (a) & (c) Result of locations to add reinforcements. (b) & (d) Result of locations to add reinforcements with material densities less than 0.1 removed.**



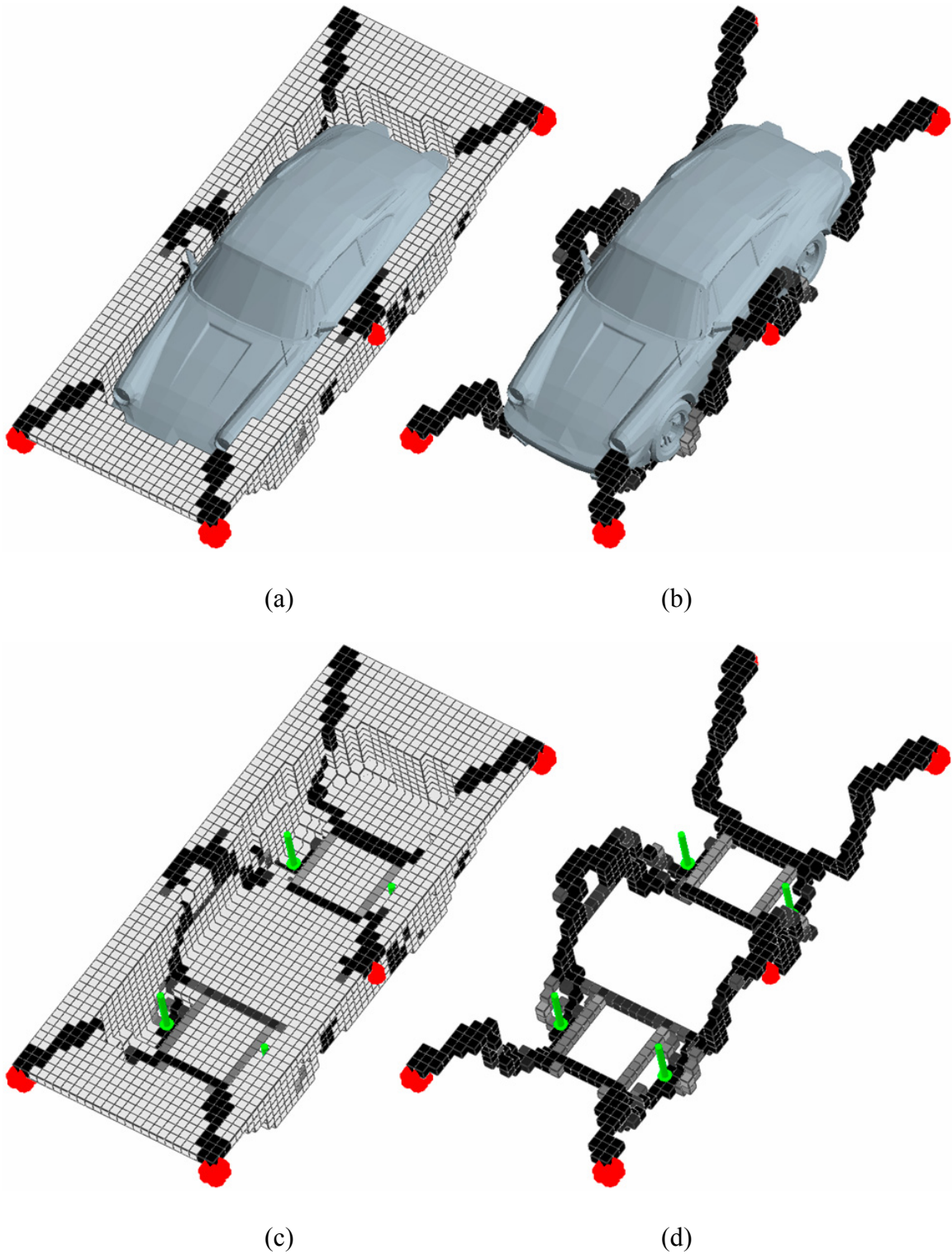


**Figure 4-12: Result of Topology Optimization for a Car Model Under Different Boundary Conditions: (a) & (c) Result of locations to add reinforcements. (b) & (d) Result of locations to add reinforcements with material densities less than 0.1 removed.**

## 4.7 Conclusion and Remarks

An automated procedure for generating reinforcement for thin-walled packaging structures has been developed in this paper. This method can identify the design space for topology optimization very efficiently and avoid many mold design problems such as undercuts. Topology optimization is applied to produce the optimal placement of reinforcement for the thin-walled structure under a mean compliance formulation. One interesting by-product of this method is that a packaging foam model is obtained immediately before generating a thin-walled design space.



## **Chapter 5.**

### **Conclusion and Future Work**

Study and research on industrial packaging are carried out and some results on three different types of packaging are presented in this dissertation. The achievement of this study is concluded in this chapter and further research can be expended based on this research is also discussed here.

#### **5.1 Conclusion**

Sustainability and environmentology have become important issues because the natural resources have been heavily consumed in the past century and a major part of them have been wasted on some one-time-use type of applications such as packaging. Design for sustainability and environmentology in industrial packaging has been described in this research. Topology optimization of packaging structures utilizing environmental friendly materials is studied in this dissertation such that less material is needed in a set of packaging while strength of the packaging structure is optimized; and less pollution and impact to the environment is accomplished.

The development of using topology optimization to packaging structures is divided into a few parts and some achievement is accomplished and stated as follows:

First, in Chapter 2, design of core structure of sandwich board is optimized based on topology optimization methods. Topology optimization methods are reviewed and

discussed. A simple variable updating scheme is composed for topology optimization process. The optimization process uses the stress simulation results obtained from finite element methods, calculates the sensitivity of element energy density, and updates the design variables for the next finite element analysis. Based on the optimality criteria, the resultant structure generated from this process is guaranteed to be the optimal topology. From the topology optimization results of applying different boundary conditions to specific design spaces of the sandwich board, it suggests that the triangular structure is the optimal one for the core of sandwich structures subject to the load and constraints simulated.

Second, in Chapter 3, an efficient algorithm of obtaining supporting surface that can be used to create molded foam or thin film container is developed. This algorithm takes a commonly used data format that describes 3D models as input and generates an evenly distributed supporting grid with height information to export an undercut free supporting surface. Because this algorithm keeps the data structure simple and clear, the efficiency is impressive and the result is accurate and valid. Three examples are used to demonstrate its efficiency and accuracy. The first ball example shows that this algorithm provides undercut free supporting surface. The second example has multiple parts and this algorithm generates valid results. The third example has a very large amount of facets and this algorithm shows its efficiency to generate accurate results. This algorithm also provides a way to determine a design space for topology optimization process for finding a good supporting structure while keeping its strength of providing undercut free spaces.

Finally, in Chapter 4, topology optimization is applied to design spaces, modified from the spaces obtained from the algorithm discussed in Chapter 3, to find locations to add reinforcements on the thin-walled design space which can be used to form molded pulp tray. The procedures first take the supporting surface generated from Chapter 2 and calculate a continuous layer of finite elements along the surface. Then apply topology optimization method discussed in Chapter 2 to find locations where reinforcements are recommended. The result depends on the boundary conditions defined to the design space which should be justified by the user. Two examples are presented in Chapter 4. The first simple box example shows the validation of this process by generating a reasonable supporting structure. The second example with complex model shows the strength of this method to handle complex objects without problem.

The study in this dissertation about utilizing topology optimization methods to optimize packaging structures extensively extends the scope of applications of topology optimization. Furthermore, this research also provides a vision of using environmental friendly materials to replace unnecessary usage of plastics which can improve the sustainability of our only Earth.

## 5.2 Future Work

Although this research suggests a way to optimize packaging structures, not all kinds of structures are studied. Some more studies can be performed on optimizing other usage of packaging structures. Some possibilities are pointed out as follows:

- *3D core structures of sandwich boards*

In Chapter 2, 2D sandwich board design space is studied and the result is used to visualize a board structure. However, it is a 2.5D structure. For finding an

optimal 3D sandwich structure can be studied more. It is likely that providing a well defined design space with appropriate boundary conditions, the 3D core structure can be found.

- ***Further applications of algorithms described in Chapter 3***

The algorithm described in Chapter 3 generates undercut free supporting surfaces. This algorithm can be used to detect parting line or parting surface of models with minor modifications. For molded parts, it is critical to define a good parting line / surface so that the products can be manufactured with higher quality. Locations that undercuts are possible to happen can be detected by the algorithm and, therefore, a different orientation of the object can be found to have less undercut; or a separate mold bulk can be defined to form the cavity of the part where undercut can be avoided.

- ***Refinement and realization of molded pulp molds***

Some further study can be applied to the result obtained from Chapter 4 to convert the structure into rid-reinforced structure such that thin wall property can be maintained and simple manufacturing process for molded pulp can be preserved.

## Bibliography

- [1] J.J. Burgiel, "Recycling rates...revisited," in *Plastics News*, 1999.
- [2] Richard A. Denison, "Something to hide - The sorry state of plastics recycling," Environment Defense Fund 1997.
- [3] R.E. Drumright P.R. Gruber, , D.E. Henton, "Polylactic acid technology," *Advanced Materials*, vol. 12, pp. 1841-1846, 2000.
- [4] V.S. Deshpande X. Qiu, , N.A. Fleck, "Finite element analysis of the dynamic response of clamped sandwich beams subject to shock loading," *European Journal of Mechanics A/Solids*, vol. 22, pp. 801-814, 2003.
- [5] N.A. Fleck, V.S. Deshpande "The resistance of clamped sandwich beams to shock loading," *Journal of Applied Mechanics* vol. 71, pp. 386-401, 2004.
- [6] J. Hohe, W. Becker, "Optimized structural sandwich panels with minimum delamination hazards," *Structural and Multidisciplinary Optimization*, vol. 23, 2002.
- [7] J.W. Hutchinson L. Valdevit, , A.G. Evans, "Structurally optimized sandwich panels with prismatic cores," *International Journal of Solids and Structures*, vol. 41, 2004.
- [8] H.A. Eschenauer, N. Olhoff, "Topology optimization of continuum structures: A review," *Applied Mechanics Review*, vol. 54, pp. 331-390, 2001.
- [9] J.C. Maxwell, "On reciprocal figure, frames, and diagrams of force," *Transactions of the Royal Society of Edinburgh*, vol. 26, 1872.
- [10] A.G.M. Michell., "The limits of economy of material in frame-structure," *Phil Mag.*, vol. 8, pp. 589-597, 1904.
- [11] Yoshimasa Tokuyama, and Seockhoon Bae, "An approximate method for generating draft on a free-form surface," *The Visual Computer*, vol. 15, pp. 1-8, 1999.
- [12] F.R. Shanley, *Weight strength analysis of aircraft structure*. New York: Dover Publications, 1960.
- [13] R.H. Gallagher, O.C. Zienkiewicz, *Optimum structure design, theory and applications*. New York: John Wiley & Sons, 1973.
- [14] W. Pager, J.E. Taylor, "Problems of Optimal Structural Design," *Journal of Applied Mechanics*, vol. 35, pp. 102~106, 1968.

- [15] C.Y. Sheu, W. Prager, "Recent development in optimal structural design," *Applied Mechanics Review*, vol. 21, pp. 985~992, 1968.
- [16] K.A. Cunefare, Z. Mroz, "Variational approach by means of adjoint systems to structural optimization and sensitivity analysis," *International Journal of Solids and Structures*, vol. 19, pp. 667~692, 1983.
- [17] K.K. Choi, E.J. Haug, "Shape design sensitivity analysis of elastic structures," *Journal of Structure of Mechanics*, vol. 11, pp. 231~269, 1983.
- [18] W.C. Carpenter, E.S. Smith, "Computational efficiency of nonlinear programming methods on a class of structural problems," *International Journal of Numerical Methods in Engineering*, vol. 11, pp. 1203~1223, 1973.
- [19] K. Schittkowski (Ed.), *Computational Mathematical Programming*. Berlin: Springer-Verlag, 1985.
- [20] A.D. Belegundu, J.S. Arora, "A study of mathematical programming methods for structural optimization. Part 1: Theory," *International Journal of Numerical Methods in Engineering*, vol. 21, pp. 1583~1599, 1985.
- [21] HAYDN N. G. WADLEY, "Multifunctional periodic cellular metals," *Philosophical Transactions of the Royal Society*, vol. 364, pp. 31-68, 2006.
- [22] G. Strang, R.V. Kohn, "Optimal design in elasticity and plasticity," *International Journal for Numerical Methods in Engineering*, vol. 22, pp. 183-188, 1986.
- [23] C.S. Jog, R.B. Haber, M.P. Bendsoe, "Variable-topology shape optimization with a control on perimeter," presented at Advances in design automation, Washington D.C., 1994.
- [24] M.P. Bendsoe, N. Kikuchi, "Generating optimal topologies and structural design using a homogenization method," *Computer Methods in Applied Mechanics and Engineering*, vol. 71, pp. 197-224, 1988.
- [25] M.P. Bendsoe, "Optimal shape design as a material distribution problem," *Structural Optimization*, vol. 1, pp. 193-202, 1989.
- [26] H.C. Gea, "A new micro structural based design domain method," *Computers and Structures*, vol. 61, pp. 781-788, 1996.
- [27] M.p. Bendsoe, O. Sigmund, "Material interpolation schemes in topology optimization," *Archive of Applied Mechanics*, vol. 69, pp. 635-654, 1999.
- [28] H. C. Gea, "Topology optimization: A new microstructure-based design domain method," *Computers and Structures*, vol. 61, pp. 781-788, 1996.

- [29] D. Jung, H.C. Gea, "Design of energy absorbing structure using topology optimization with a multi-material model," presented at DETC, 2003.
- [30] H. C. Gea, "Topology Optimization: A New Micro-Structural Based Design Domain Method," *Computers and Structures*, vol. 61, pp. 781-788, 1996.
- [31] V.S. Deshpande, N.A. Fleck, "Collapse of truss core sandwich beams in a 3-point bending," *International Journal of Solids and Structures*, vol. 38, pp. 6275-6305, 2001.
- [32] L. A. Carlsson, "On the elastic stiffnesses of corrugated core sandwich," *Journal of Sandwich Structures And Materials*, vol. 3, pp. 253-267, 2001.
- [33] M. W. FU, J. Y. H. FUH, and A. Y. C. NEE, "Core and cavity generation method in injection mould design," *Int. J. Prod. Res.*, vol. 39, pp. 121-138, 2001.
- [34] M.W. Fu, J.Y.H. Fuh, and A.Y.C. Nee, "Generation of optimal parting direction based on undercut features in injection molded parts," *IIE Transactions*, vol. 31, pp. 947-955, 1999.
- [35] T. Wong, S. T. Tan, and W. S. Sze, "Parting line formation by slicing a 3D CAD model," *Engineering with Computers*, vol. 14, pp. 330-343, 1998.
- [36] Alok K. Priyadarshi, and Satyandra K. Gupta, "Geometric algorithms for automated design of multi-piece permanent molds," *Computer Aided Design*, vol. 36, pp. 241-260, 2004.
- [37] C. L. Li, "Application of Catmull-Clark subdivision method in plastic injection mould parting surface design," presented at The Sixth International Conference on Information Visualisation, London, England, 2002.
- [38] Jayanth Majhi, Prosenjit Gupta, and Ravi Janardan, "Computing a flattest, undercut-free parting line for a convex polyhedron, with application to mold design," *Computational Geometry*, vol. 13, pp. 229-252, 1999.
- [39] Xiuzhi Qu, and Brent Stucker "A 3D surface offset method for STL-format models " *Rapid Prototyping Journal* vol. 9, pp. 133-141, 2003.
- [40] H.B. Jung, and K. Kim, "A new parameterization method for NURBS surface interpolation," *The International Journal of Advanced Manufacturing Technology*, vol. 16, pp. 784-790, 2000.
- [41] S.M. Hu, Y.F. Li, T. Ju, and X. Zhu, "Modifying the shape of NURBS surfaces with geometric constraints," *Computational Geometry*, vol. 33, pp. 903-912, 2001.

- [42] C.K. Chua K.F. Leong, and Y.M. Ng, "A study of stereolithography file errors and repair. Part 1. Generic solution," *The International Journal of Advanced Manufacturing Technology* vol. 12, pp. 407-414, 1996.
- [43] Danny G. Eagleton, Jorge A. Marcondes, "Cushioning properties of moulded pulp," *Packaging Technology and Science*, vol. 7, pp. 65-72, 1994.
- [44] G. Wang, C. Fu, "Investigation on design of molded pulp cushioning products," *China Pulp and Paper*, vol. 20, pp. 25-28, 2001.
- [45] John Hoffmann, "Compression and cushioning characteristics of moulded pulp," *Packaging Technology and Science*, vol. 13, pp. 211-220, 2000.
- [46] Tsutomu Noguchi, Mayumi Miyashita, "Development of moulded pulp materials for the packaging of electronic equipment," *Packaging Technology and Science*, vol. 10, pp. 161-168, 1997.
- [47] MSC Nastran, *Getting started with MSC.Nastran User's Guide*: MSC Nastran, 2001.
- [48] H. C. Gea, J Luo., "On stress based and strain based method for prediction of optimal orientation of orthotropic materials," *Structural and Multidisciplinary Optimization*, vol. 26, pp. 229-234, 2004.
- [49] J. Luo, H. C. Gea, "Optimal orientation of orthotropic materials using an energy based method," *Journal of Structural Optimization*, vol. 15, pp. 230-235, 1998.
- [50] P. Pedersen, "On thickness and orientational design with orthotropic materials," *Structural and Multidisciplinary Optimization*, vol. 3, pp. 69-78, 1991.
- [51] P. Pedersen, "Bounds on elastic energy in solids of orthotropic materials," *Structural and Multidisciplinary Optimization*, vol. 2, pp. 55-63, 1990.
- [52] P. Pedersen, "On optimal orientation of orthotropic materials," *Structural and Multidisciplinary Optimization*, vol. 1, pp. 101-106, 1989.
- [53] J. Luo, H. C. Gea, "Optimal stiffener design for interior sound reduction using a topology optimization based approach," *ASME Journal of Vibration and Acoustics*, vol. 125, pp. 267-273, 2003.
- [54] H. C. Gea, J Luo., "Automated optimal stiffener pattern design," *International Journal of Mechanics of Structures and Machines*, vol. 27, pp. 275-292, 1999.
- [55] J. Luo, H. C. Gea, "Optimal bead orientation in 3D shell/plate structures," *Finite Elements in Analysis and Design*, vol. 31, pp. 51-71, 1998.
- [56] J. Luo, H. C. Gea, "A systematic topology optimization approach for bead pattern design," *Journal of Structural Optimization*, vol. 16, pp. 280-288, 1998.



- [57] J. Luo, H. C. Gea, "Optimal stiffener design for interior sound reduction," *SAE Transactions, Journal of Passenger Cars*, No. 971542, 1997.
- [58] H. C. Gea, Y. Fu, "Optimal 3-D stiffener design with frequency considerations," *Advances in Engineering Software*, vol. 28, pp. 525-531, 1997.
- [59] H. C. Gea, Y. Fu, "3-D shell topology optimization using a design domain method," *SAE Transactions, Journal of Passenger Car*, No. 951105, vol. 104, pp. 1983-1989, 1995.
- [60] H. Chickermane, H. C. Gea, "Structural optimization using a new local approximation method," *International Journal for Numerical Methods in Engineering*, vol. 39, pp. 829-846, 1996.

# Curriculum Vita

## Ching-Jui Chang

- 1994 – 1998 B.S., Depart of Mechanical Engineering, National Central University, Chung-Li, Taiwan.
- 1998 – 2000 M.S.E., Automation and Control Engineering Program, National Taiwan University of Science and Technology, Taipei, Taiwan.
- 2000 – 2002 Research Assistance, Depart of Computer Science and Information Technology, National Taiwan University, Taipei, Taiwan.
- 2004 – 2007 CAD Instructor, Department of Mechanical and Aerospace Engineering, Rutgers, The State University of New Jersey, New Brunswick, New Jersey.
- 2002 – 2007 Ph.D., Department of Mechanical and Aerospace Engineering, Rutgers, The State University of New Jersey, New Brunswick, New Jersey.

### Publications:

1. Ching-Jui Chang, Bin Zheng, Hae Chang Gea, “Topology Optimization for Tension/Compression Only Design“, *7<sup>th</sup> World Congress on Structural and Multidisciplinary Optimization*.
2. Ching-Jui Chang, Hae Chang Gea, “Automated Design of Thin-walled Packaging Structures”, *Journal of Structural and Multidisciplinary Optimization*, In Press.
3. Ching-Jui Chang, Hae Chang Gea, “An Efficient Method for Detecting Packaging Supporting Space”, *32<sup>nd</sup> Design Automation Conference in IDETC 2006*.
4. N.N. Puri, S. Al-Takroui, C. Chang, I. Yasar, “Optimal Three Mode Controller for the High Order Time Delay Systems”, *The ninth IASTED Internal Conference on Intelligent Systems and Control, 2006. Page 168-173*.
5. Ching-Jui Chang, Po-Ting Lin, Bin Zheng, Jack Wang, “Compliant Mechanism Based material Design using Micro-Molding”, *ASME Graduate Student Mechanism Design Competition, 31st Design Automation Conference in IDETC 2006*.
6. C.J. Chang, “Research of a Mask-based Curing Technique for Rapid Prototyping System Development”, *National Taiwan University of Science and Technology, Master Thesis, 2000*.
7. C.J Chang and M.J Tsai, “A Mask-based Curing Technique for Rapid Prototyping System Development”, *The Sixth International Conference on Automation Technology, 2000. Proceeding Vol.1, pp637-642*.
8. C.J Chang and M.J Tsai, “Research of Electronic mask-based rapid prototyping control interface design”, *The first cross-strait workshop on manufacturing technology. 2000. Page184-191*.